ISSN 0280-5316
ISRN LUTFD2/TFRT--5771--SE

Tire-Road Friction Estimation Using Slip-based Observers

Mathieu Gerard

Department of Automatic Control
Lund University
June 2006

Department of Automatic Control
Lund Institute of Technology
Box 118
SE-221 00 Lund Sweden

Document name
MASTER THESIS

Date of issue
June 2006

Document Number
ISRN LUTFD2/TFRT--5771--SE

Author(s)
Mathieu Gerard

Supervisor
Anders Rantzer and Brad Schofield at Automatic Control Lund, Sweden.
Rodolphe Sepulchre at BAT Systèmes et Modélisation Liège, Belgium.

Sponsoring organization

Title and subtitle
Tire-Road Friction Estimation Using Slip-based Observers (Friktionsuppskattning mellan väg och däck genom sladd-baserade observerare)

Abstract

In order to improve the security of the vehicles, the car industry focuses more and more on Active Safety. The objective is to introduce embedded electronic control systems to detect dangerous conditions, warn the driver and, in emergency situations, even take actions to avoid crash or at least reduce the violence of the impact. The tire-road friction coefficient which defines the maximum traction and braking capacities is very useful information for both the driver and electronic devices like ABS, ESP, roll-over prevention or collision mitigation. Unfortunately such a coefficient cannot be directly measured and has to be estimated from other available data. This thesis reviews the main directions followed by researchers around the world and then focuses on slip-based methods. The methods proposed in a few papers are implemented, compared and commented. Then some original solutions are proposed.

First, a hybrid observer has been developed with the idea to classify roads into a few categories. The principle is very interesting and the implementation brings out many problems to take into consideration and some attempts of solutions.Secondly, a force observer and a tire friction model are combined. This natural approach works well in simulations.

Keyword
Tire-road friction estimation, slip-based methods, hybrid observer, Unscented Kalman Filter, nonlinear friction model. s

Classification system and/or index terms (if any)

Supplementary bibliographical information

ISSN and key title	*ISBN*
0280-5316	

Language	*Number of pages*	*Recipient's notes*
English	66	
Security classification		

The report may be ordered from the Department of Automatic Control or borrowed through:University Library, Box 3, SE-221 00 Lund, Sweden Fax +46 46 222 42 43

Acknowledgment

This year of study and research as an Exchange Student in Lund has been a very wonderful experience. First of all I would like to thank all the professors, PhD students and staff of the Automatic Control department. For the help in big and small problems, for the sports, for the fun, for the numerous fika... tack så mycket till alla!

From a technical point of view, a particular thank you to my two supervisors. Thanks Brad for making yourself available, for your motivation and your good advice. Our discussions were enriching and had me return to my work with clearer ideas. Thanks also to Prof. Anders Rantzer for having been a source of inspiration. I really appreciated the way you helped me defining the main directions of my project while leaving me the liberty to search for interesting areas.

I would also like to thank the team at Modelon for the course about Modelica and the support concerning the Vehicle Dynamics Library.

Finally, merci beaucoup to Prof. Rodolphe Sepulchre for having initiated the partnership with Lund and for handling the administrative tasks in Liège.

Contents

Chapter 1

Introduction

Except in the centre of Lund, this small and beautiful university city in southern Sweden where Swedes and Exchange Students use bikes, cars have become the most popular and easiest way to move and travel. Unfortunately, even with all the mechanical improvements made by the manufacturers, this way of transport is still quite dangerous and causes a lot of injuries every day all around the world. One direction taken by the industry to reduce the number of crashes and their seriousness is to develop Active Safety systems: embedded electronic systems that detect critical conditions to warn the driver and/or induce some actions directly on the brakes, the engine, the steering or any other available actuator.

Some of those systems are already present on the market and well known to the public.

A first one is the Anti-lock Braking System (ABS) which helps the car to stop on a shorter distance in case of emergency braking while maintaining steering capabilities for the driver. The basic idea is to avoid wheel lock by modulating the brake torque. This idea relies on the fact that the friction between the tire and the road as well as the steering capabilities are inferior when the wheel is sliding instead of rolling. The new generation of ABS systems will go a bit further and optimize the braking by trying to use the maximum of the friction curve (further details later on).

The Electronic Stability Program (ESP) is another device that adjust brake forces and driving torque to maintain the vehicle in controllable limits and avoid under-, oversteer or even spinning.

Roll-over prevention and collision mitigation are other examples currently under research. Many other systems are going to appear in the next few years, not to take the control of the vehicle or become the main driver, but to warn and assist the human driver in case of inattention or critical manoeuvres.

Of course, to be able to do something interesting, any system needs information, and the more information it gets, the more accurate and optimal it can perform. For that purpose, cars are equipped with sensors that measure some elements of the dynamics of the body. Sensors being expensive, the best is to use as few as possible and extract all the available information through cheaper algorithms. Some information that could be very useful is not measurable or the price for it would be much too high. It is therefore needed to design specific observers to get an estimate of the unknown variables using measurements coming from elsewhere.

The friction coefficient between the tire and the road is exactly the kind of information which is very useful but not directly measurable. This thesis focuses on that problem and presents some existing and new ideas to estimate the friction, or to be more precise, the maximum available friction μ_{max}.

Most of the time researchers try to classify the road in categories like dry asphalt, wet asphalt, gravels, snow, ice, etc [7] [8] [11]. The availability of that information can be very useful both to warn the driver in case of slippery road and to tune other control systems. For example, it is known that the friction against the road presents a maximum for a given ratio between the longitudinal and angular speed of the wheel. This ratio depends on the kind of road. If the road is known, the ABS controller can use that information to stabilize the wheel's speed at that specific ratio and so maximize the braking efficiency. Another application would be to be able to estimate the braking capabilities we can expect from the present driving conditions and use them as constraints in control signals from systems like ESP. The knowledge of the braking capacities also allow a comparison between the deduced braking distance and the position of obstacles detected by an embedded radar. As well, if the friction forces are estimated during the process they can allow the closing of an inner control loop for other control systems like in roll-over prevention and check that the actual action agrees with the requested one.

This very promising subject seems unfortunately very difficult to handle. Many researchers are working on it all around the world and a huge amount of papers have already been published. However no one has really found yet a miraculous solution. This thesis does not have the ambition to revolutionize the area but to learn how to enter and contribute to a very interesting research topic.

1.1 Purpose and objectives

The objective of this thesis is to discover the research, as well as to apply the theory learned during the studies, to learn new methods and to develop skills in the control and estimation field.

In more details, the main steps are :

- Understand the problem of friction estimation
- Learn advanced methods that seem to be useful
- Look for existing solutions and propositions, try some implementations and comment approaches
- Propose new ideas and
  - ⋆ Implement them
  - ⋆ Simulate them
  - ⋆ Investigate their robustness
  - ⋆ Conclude on the interest, advantages and drawbacks

1.2 Practical details and software

The entire work has been done at the department of Automatic Control of Lund University in Sweden within the context of an ERASMUS exchange, under the supervision of Prof. Anders Rantzer and Brad Schofield.

Simulations have been performed using the Vehicle Dynamics Library developed by Modelon AB [1]. This library uses the Modelica [2] modelling language to describe a very detailled model of a complete car. Modelica is an open-standard object-oriented equation-based modelling language designed for effective component-oriented modelling of complex systems.

The interpretation and solving of the Modelica models has been done using Dymola, Dynamic Modeling Laboratory, developed by Dynasim AB [3].

Moreover, Matlab [4] has been used to analyze the simulation results as well as to implement and develop some filters.

1.3 Outline

The first part of this thesis gives the background of the theory developed in the next sections. Chapter 2 focuses on the automotive background by introducing the vehicle's model, the frames, the parameters, the tire friction model and the manoeuvres. While Chapter 3 details the Kalman Filter and its nonlinear extensions.

Chapter 4 presents the state-of-the-art of tire-road friction estimation and introduces the slip-based methods.

[1] http://www.modelon.se (Ideon, Lund, Sweden)
[2] http://www.modelica.org
[3] http://www.dynasim.se (Ideon, Lund, Sweden)
[4] http://www.mathworks.com

Chapter 5 and 6 explain in more details two slip-based methods found in the literature and show some simulation tests.

The two last chapters describe original ideas investigated during this work and gives appreciations based on simulations. The first idea is based on hybrid observers and the second merges and extends the methods of chapters 5 and 6.

Finally, a conclusion and some suggestions relative to further development are presented.

Chapter 2

Automotive Background

2.1 The vehicle model

A particularity that makes the vehicle model quite complex and complicated is the multiplicity of references and systems of coordinates called frames. All frames are based on the "right hand rule" and oriented so that x is directed towards the front, y towards the left and z towards the top. The most important frames are :

- **The World frame** : a static system of coordinates that does not move during the experiment. The gravity's acceleration is in the direction of $-z$.
- **The Vehicle frame** : the system of coordinates is attached and moves with the vehicle. The x axis points to the front, the y to the left side and z to the roof.
- **The Wheel frame** : the system of coordinates is attached at the contact point between the tire and the road. The z axis is normal to the road and y follow to the left the rotation axis of the wheel.

A move is said **longitudinal** along the x axis and **lateral** along the y axis. The rotations are called **roll** around x, **pitch** around y and **yaw** around z.

As it is the tradition, different conventions exist in Europe and in the US. Here the European version is presented and used. To convert the models to the American standard one just has to keep the x axis and turn over the y and z axis (y to the right and z to the bottom). That just implies some terms to get a minus sign ... the game is to know which one :-)

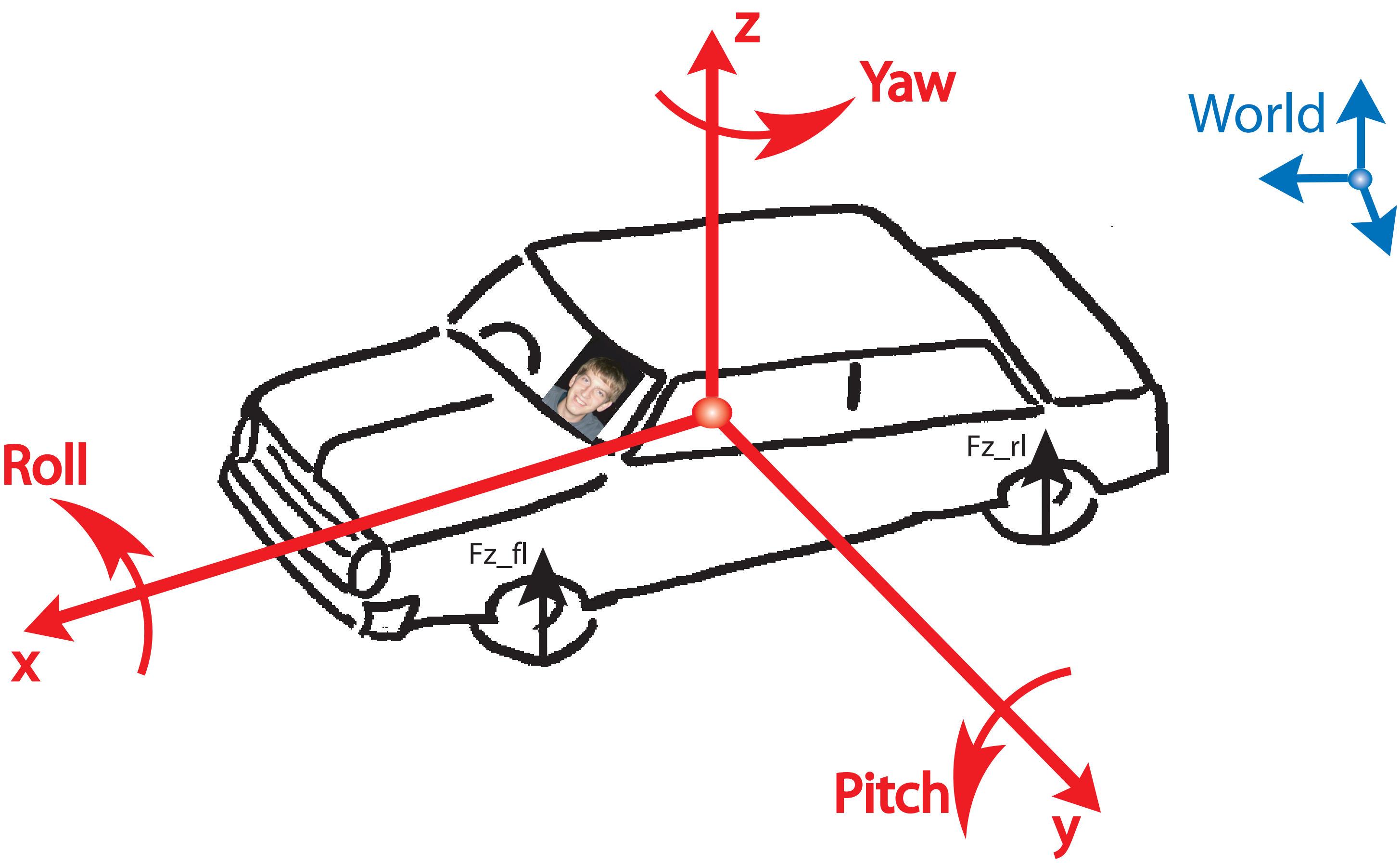

Figure : World and Vehicle frames

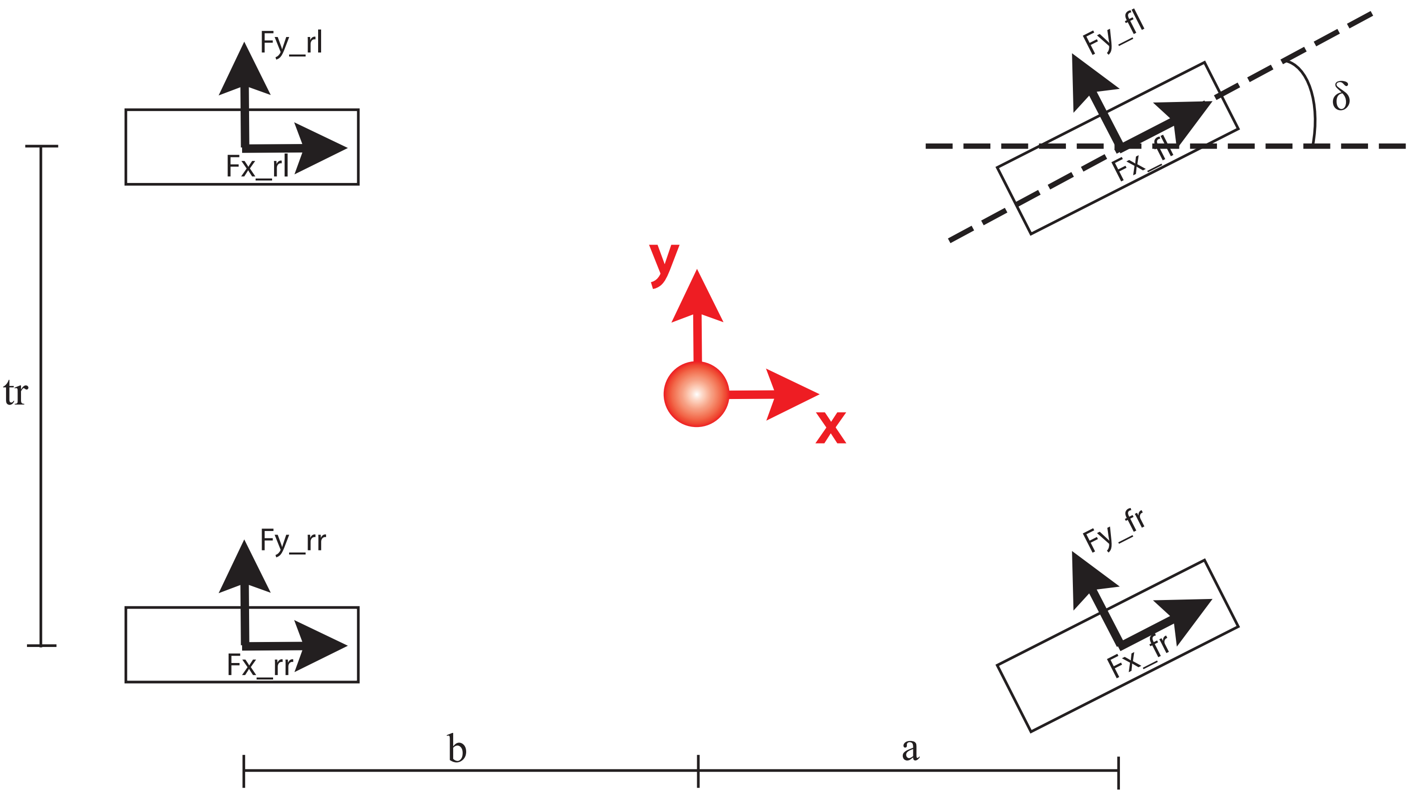

Figure : Vehicle and Wheel frames

To simplify the understanding of the equations and the juggling between the frames, I set a convention through this report : the variables that start with a capital letter are expressed in the wheel frame. The others are related to the vehicle frame.

The basic equations describing the dynamics of the vehicle are :

$$
\begin{aligned}
a_x &= \frac{1}{m}[((Fx_{\text{fl}} + Fx_{\text{fr}})\cos(\delta)) - ((Fy_{\text{fl}} + Fy_{\text{fr}})\sin(\delta)) + (Fx_{\text{rl}} + Fx_{\text{rr}})] \\
a_y &= \frac{1}{m}[((Fx_{\text{fl}} + Fx_{\text{fr}})\sin(\delta)) + ((Fy_{\text{fl}} + Fy_{\text{fr}})\cos(\delta)) + (Fy_{\text{rl}} + Fy_{\text{rr}})] \\
\frac{dr}{dt} &= \frac{1}{Izz}[((Fx_{\text{fl}} + Fx_{\text{fr}})a\sin(\delta)) + ((Fy_{\text{fl}} + Fy_{\text{fr}})a\cos(\delta)) - (Fy_{\text{rl}} + Fy_{\text{rr}})b - \\
&\quad ((Fx_{\text{fl}} - Fx_{\text{fr}})\cos(\delta))\frac{tf}{2} - ((Fx_{\text{rl}} - Fx_{\text{rr}}))\frac{tr}{2})
\end{aligned}
$$

$$
\begin{aligned}
a_x &= \dot{v_x} - v_y r \\
a_y &= \dot{v_y} + v_x r
\end{aligned}
$$

Where

v	speed of the car body
V	speed of the tire-road contact point
a	acceleration
r	yaw rate
F	force
δ	steering angle
ω	angular speed

The wheels are referred by the indices

fl	front left
fr	front right
rl	rear left
rr	rear right

The parameters describing the vehicle are :

Letter	Name	Typical value
a	distance from CoG to front axel	1 m
b	distance from CoG to rear axel	1.5 m
tf	front track width	1.5 m
tr	rear track width	1.5 m
Izz	inertia around z axis for yaw movement	1300 kgm^2
m	mass of the vehicle	1300 kg
R	radius of the wheels	0.28 m

An interested reader can refer to Rill [1] and Gillespie [2] for more detailled considerations about vehicle dynamics.

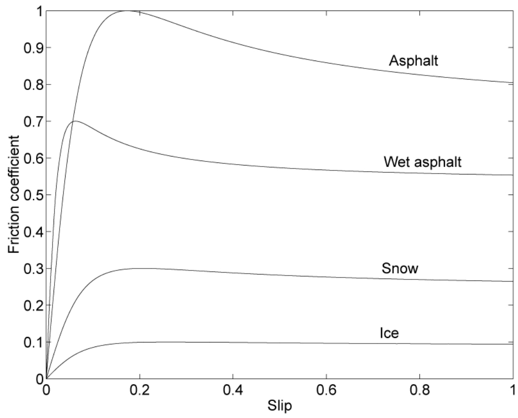

Figure 2.1: Slip curves with exaggerated characteristics extracted from [11]. The maximum available friction, as well as the position of the maximum and the initial slope, varies depending on the type of road.

2.2 Tire models and slip

There are a lot of ways to model a tire. Some are based on detailed physical modelling while other are based on characteristic functions. A good summary of many available models can be found in [5]. Most of the models define the friction μ, the ratio between the friction forces and the vertical force, as a function of a quantity λ called *slip* and defined as

$$\mu = \frac{Fx}{Fz} = \mu(\lambda)$$

$$\lambda = \frac{V_x - R\omega}{V_x}$$

Tire "slip" occurs whenever pneumatic tires transmit forces. The slip ratio express the relative difference between the longitudinal speed V_x and the rolling speed $R\omega$ at the contact point. A free rolling wheel has a zero slip while a sliding wheel has a unity slip.

The curves showing the relation between the friction and the slip for different kind of roads are shown on figure 2.1. This picture is directly extracted from [11]. Note that some of the characteristics like the slopes for low slip have been weakly exaggerated.

We can clearly see a maximum in the curves, at least for not too slippery roads. The maximum friction available on a given road is called μ_{max}. That's the most important value to estimate since it describes how much we can expect from the present driving condition, for example the maximum braking force.

In all the cases, the friction for a sliding wheel ($\lambda = 1$) is less than the friction for a rolling one. We have now the justification of the improvement brought by the ABS system that reduces, if necessary, the brake pressure to avoid a wheel lock and maintain a higher friction level.

Without entering in the details, we can mention that for low slips, before the maximum of the curve, the system is stable. An augmentation of the slip will give a higher friction that will tend to reduce the slip. However, for large slips, after the maximum, a higher slip will reduce the friction and the slip will increase again. The system becomes therefore unstable and lead to wheel lock.

One of the most famous and used empirical model is the Magic Formula developed by Pacejka [3]. The main idea is to model the curve by an equation of the form :

$$y(x) = D \sin[C \arctan\{Bx - E(Bx - \arctan(Bx))\}]$$

With some parameters depending on the wheel load :

D	Peak value
C	Shape factor
B	Stiffness factor
E	Curvature factor

For low slip, the model can be seen as a linear one with the longitudinal stiffness C_x defined as the slope of the curve :

$\mu = C_x \lambda$

Depending on the authors and the articles it appears or not that this longitudinal stiffness C_x contains information about μ_{max}. Actually, in all the articles that uses linear regression to estimate C_x from measured data, the researchers manage to show a direct link between the slope and the maximum of the curve, for example in Gustafsson [11] and Uchanski [7]. At the converse, while using physical tire models or doing specific experiments, it clearly seems that the stiffness depends much more on tire parameters like material, temperature, load, pressure and tread instead of the road property. Numerous tests and results can be found in Carlson and Gerdes [4].

So a linear model for low slip seems not so obvious to use. Anyway, since it has been used successfully by some authors, such an approach will stay conceivable as explained in [7].

2.3 Simulations and Manoeuvres

In next sections, the implementations of the observers will be tested on simulations. This section describes how the simulations are made and what manoeuvres are used.

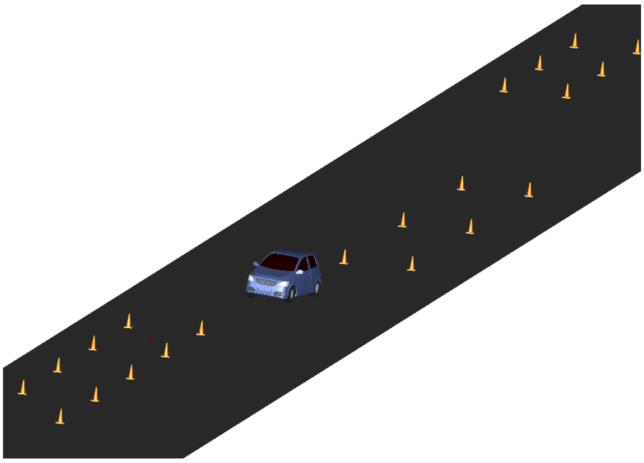

Figure 2.2: Picture of the Double Lane Change and Braking manoeuvre. The car slaloms between the cones and starts braking just after entering the last set of cones.

Using the Vehicle Dynamics Library for Modelica, the model of a complete car is created as well as a road. A driver is added and programmed to execute a specific manoeuvre. Basically, the vehicle used is close to the one proposed as an example in the Library. The complete model is then simulated and all the results (time-varying variables) are stored in a mat file. Once it is done, the needed variables are loaded in the Matlab workspace and the Matlab algorithm is run to get and plot the estimated values.

Two manoeuvres with different characteristics will be used in order to demonstrate different behaviours: *Double Lane Change and Braking* and *Straight Line Acceleration and Braking*.

Both simulations are run for 10 seconds but each time a transient is removed. Of course in real life the time scale would be much larger but it seems clear than a few seconds are enough to capture the main behaviour of the filters.

2.3.1 Double Lane Change and Braking

During the Double Lane Change and Braking manoeuvre, the vehicle will first swerve to the left like a lane change. Then the same movement is made to the right. When back on the initial lane, a heavy braking is engaged. Figure 2.2 shows a picture of the road where the cones describe the car's trajectory.

To clarify the ideas, the absolute lateral displacement of the car on the road and the absolute longitudinal speed are displayed on figure 2.3. Note that absolute means in a system of coordinate attached to the road with always x to the front and y to the left.

This manoeuvre can be considered quite extreme, at least it is not usual in

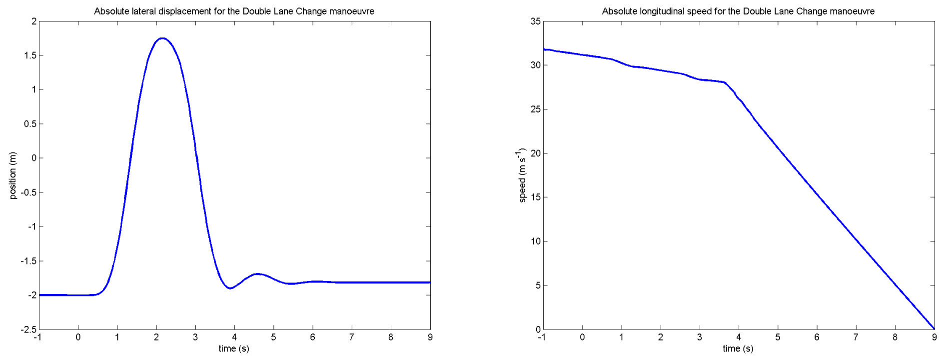

Figure 2.3: Details of the Double Lane Change and Braking manoeuvre. The absolute lateral displacement, displayed on the left, shows the slalom between the two lanes. The absolute longitudinal velocity, plotted on the right, first decreases slowly because of the drag and rolling resistances, before the heavy braking.

everyday driving. Moreover it proposes a quite good excitation of the steering at the beginning and of the braking at the end.

The road friction coefficient available as parameter in the Modelica road model is always set to 1.

The negative time indicate that the first moments will be removed from the filtering due to the transient taking place at the beginning of the simulation.

2.3.2 Straight Line Acceleration and Braking

The Straight Line Acceleration and Braking manoeuvre has the particularity not to excite the steering dynamic at all and to have a road section with lower friction. This is very close to the driving on highway where a section of the road is wet. As can be seen on figure 2.4, the vehicle is accelerated using a step between times 1 and 6 and then slowed down from time 6.5 until the end. The lower friction spot with a coefficient of 0.7 instead of 1 is reached after 4 seconds and left 4 seconds later.

When the driver is not pushing the accelerator pedal, the rolling and the engine resistances induce the deceleration observed at the beginning.

Since the vehicle is driven by 2 front wheels, the traction forces will be applied on the front wheels only and the rear wheels will only be subject to rolling resistance during the acceleration period. That non-equal distribution of the forces allows the analysis of some particular characteristics of the algorithms.

The acceleration and braking applied in this case are quite reasonnable, and the road friction is not too low, so the slip will keep quite low values which allow

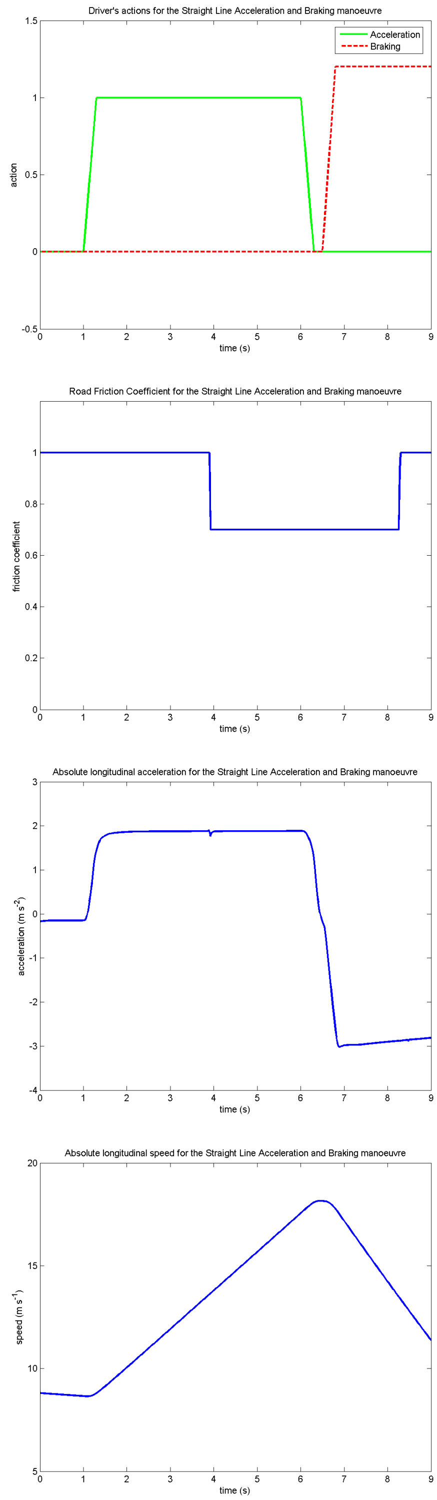

Figure 2.4: Details of the Straight Line Acceleration and Braking manoeuvre. The driver first accelerates before starting braking. The road presents a lower friction patch between the fourth and eighth second, as shown on the second picture.

us to use it to test algorithms with linear friction models.

For simplicity, the first second transient due to the engagement of the gear has been removed.

Chapter 3

The Kalman Filter and its extensions

3.1 The linear Kalman Filter

Let's consider a general estimation and filtering problem for a linear model expressed in State Space form :

$$x_{k+1} = Ax_k + Bu_k + v_k \quad (3.1)$$
$$y_k = Cx_k + Du_k + e_k \quad (3.2)$$

We assume the noisy input-output data $\{y_k\}$ and $\{u_k\}$ to be the only data available. The state x_k is not available for measurement. The noises v_k and e_k should have zero mean. The problem of optimal estimation of x_k based on input-output data and knowledge of the model can be solved by minimizing the loss function :

$$J(\hat{x}_k) = E\{(\hat{x}_{k+1|k} - x_{k+1})^2\}, \ \forall k \quad (3.3)$$

under the constraint of the measurement equation 3.2.

A recursive estimation for x_k can be expressed in the form

$$\hat{x}_{k+1} = (\hat{x}^-_{k+1}) + K_k(y_k - (\hat{y}^-_k)) \quad (3.4)$$

where $\hat{x}^-_k$ is the prediction of x_k, $\hat{y}^-_k$ is the prediction of y_k and K_k is the Kalman Gain. Assuming the prior estimate $\hat{x}_k$ and the current observation y_k to be Gaussian random variables, the optimal solution to problem 3.3 is given by the equations :

$$\hat{x}^-_{k+1} = A\hat{x}_{k|k-1} + Bu_k \quad (3.5)$$

$$\hat{y}_k^- = C\hat{x}_{k|k-1} + Du_k \tag{3.6}$$
$$\tag{3.7}$$
$$K_k = AP_kC^T(R_2 + CP_kC^T)^{-1} \tag{3.8}$$
$$P_{k+1} = AP_kA^T + R_1 - AP_kC^T(R_2 + CP_kC^T)^{-1}CP_kA^T \tag{3.9}$$
$$R_1 = E\{vv^T\} \tag{3.10}$$
$$R_2 = E\{ee^T\} \tag{3.11}$$
$$P_0 = E\{x_0x_0^T\} \tag{3.12}$$

The computation of the Kalman Gain is one the most important and critical part of the algorithm. There the assumption that the variables are Gaussian random variables is important and the equations represent the propagation of those Gaussian random variables through the dynamic of the system.

3.2 Extension to the non-linear case

In the non-linear case a general state space model has the form

$$x_{k+1} = F(x_k, u_k, v_k) \tag{3.13}$$
$$y_k = H(x_k, u_k, n_k) \tag{3.14}$$

Of course, the linear Kalman Filter can not been directly applied and many methods have been presented. Basically, the recursive equation can still be used since no assumptions were made in its development. However, the optimal expressions for the predicted state and output now take the more general forms:

$$\hat{x}_{k+1}^- = E\{F(\hat{x}_{k|k-1}, u_k, v_k)\} \tag{3.15}$$
$$\hat{y}_k^- = E\{H(\hat{x}_{k|k-1}, u_k, e_k)\} \tag{3.16}$$
$$K_k = P_{x_ky_k}P_{\tilde{y}_k\tilde{y}_k}^{-1} \tag{3.17}$$

with $\tilde{y}_k = y_k - \hat{y}_k^-$ the error of the output prediction and P defining the covariance matrix between its two indices. Those equations are not easy to compute and most of the time not possible at all to calculate without approximation. The first approximation possible and now commonly used is to simply take functions of the prior means to avoid expectations and to linearize the model at each step around the point computed the step before to propagate the Gaussian random variables. This is called the Extended Kalman Filter.

The state and output prediction are simply computed using the non-linear model

$$\hat{x}_{k+1}^- = F(\hat{x}_{k|k-1}, u_k, 0) \tag{3.18}$$
$$\hat{y}_k^- = H(\hat{x}_{k|k-1}, u_k, 0) \tag{3.19}$$

And the same equations as in the linear case are used to compute K_k where A, B, C and D now represent the linearized system around $\hat{x}_{k|k-1}$.

As such, the Extended Kalman Filter can be viewed as providing "first-order" approximations to the optimal terms. These approximations can introduce large errors in the true posterior mean and covariance of the transformed Gaussian random variables, which may lead to sub-optimal performance and sometimes divergence of the filter. Versions of the Extended Kalman Filter approximating the optimal terms to the second order exist but their increased implementation and computational complexity tend to prohibit their use.

3.3 The Unscented Kalman Filter

In their paper entitled "A New Extension of the Kalman Filter to Nonlinear Systems", Julier and Uhlmann [13] present the Unscented Kalman Filter which will be described here.

The same recursive equation and the same prior means approximations as before are used. However, the way the Gaussian random variables are propagated through the nonlinear system is quite different.

The state distribution is again represented by a Gaussian random variable, but is now specified using a minimal set of carefully chosen sample points. The statistical properties of these sample points completely capture the true mean and covariance of the Gaussian random variable; and when propagated through the true non-linear system, capture the posterior mean and covariance accurately to the 3rd order (Taylor series expansion) for any nonlinearity. To elaborate on this, we start by first explaining the unscented transformation. The Unscented Transformation is a method for calculating the statistics of a random variable which undergoes a nonlinear transformation [14].

Consider propagating a random variable x (dimension L) through a nonlinear function, $y = g(x)$. Assume x has mean $\bar{x}$ and covariance P_x. To calculate the statistics of y, we form a matrix X of $2L + 1$ *sigma* vectors X_i (with corresponding weights W_i), according to the following:

$$\begin{aligned}
X_0 &= \bar{x} \\
X_i &= \bar{x} + (\sqrt{(L+\lambda)P_x})_i & i &= 1, ..., L \\
X_i &= \bar{x} - (\sqrt{(L+\lambda)P_x})_{i-L} & i &= L+1, ..., 2L \\
W_0^{(m)} &= \lambda/(L+\lambda) \\
W_0^{(c)} &= \lambda/(L+\lambda) + (1 - \alpha^2 + \beta \\
W_i^{(m)} &= W_i^{(c)} = 1/(2(L+\lambda)) & i &= 1, ...2L
\end{aligned} \quad (3.20)$$

where $\lambda = \alpha^2(L+\kappa) - L$ is a scaling parameter. α determines the spread of the sigma points around $\bar{x}$ and is usually set to a small positive value (e.g., 1e-3). κ is a secondary scaling parameter which is usually set to 0, and β is used to incorporate prior knowledge of the distribution of x (for Gaussian distributions, $\beta = 2$ is optimal). $(\sqrt{(L+\lambda)P_x})_i$ is the ith row of the matrix square root. These sigma vectors are propagated through the nonlinear function g,

$$Y_i = g(X_i), \; i = 0, ..., 2L \quad (3.21)$$

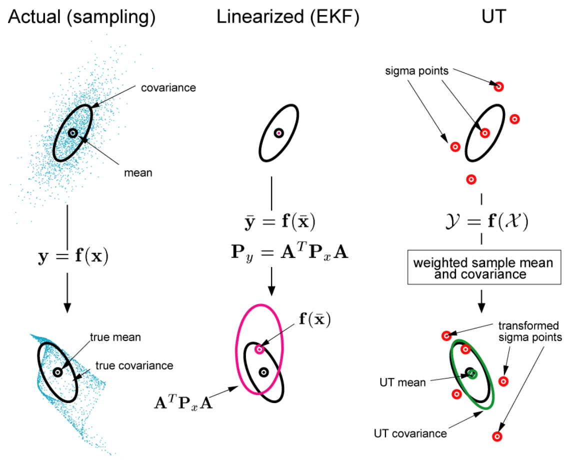

Figure 3.1: Example of the Unscented Transformation for mean and covariance propagation extracted from [14]. In the UT case, only 5 sigma points, and no linearization, are needed to propagate accurately the Gaussian random variable.

and the mean and covariance for y are approximated using a weighted sample mean and covariance of the posterior sigma points,

$$\bar{y} \approx \sum_{i=0}^{2L} W_i^{(m)} Y_i \tag{3.22}$$

$$P_y \approx \sum_{i=0}^{2L} W_i^{(c)} (Y_i - \bar{y})(Y_i - \bar{y})^T \tag{3.23}$$

Note that this method differs substantially from general "sampling" methods (e.g., Monte-Carlo methods such as particle filters) which require orders of magnitude more sample points in an attempt to propagate an accurate (possibly non-Gaussian) distribution of the state. The deceptively simple approach taken with the Unscented Transformation results in approximations that are accurate to the third order for Gaussian inputs for all nonlinearities. For non-Gaussian inputs, approximations are accurate to at least the second-order, with the accuracy of third and higher order moments determined by the choice of α and β. A simple example is shown in figure 3.1 for a 2-dimensional system: the left plot shows the true mean and covariance propagation using Monte-Carlo sampling; the center plots show the results using a linearization approach as would be done in the Extended Kalman Filter; the right plots show the performance of the Unscented Transformation (note only 5 sigma points are required). The superior performance of the Unscented Transformation is clear.

The Unscented Kalman Filter (UKF) is a straightforward extension of the Unscented Transformation to the recursive estimation in Equation 3.4, where the state RV is redefined as the concatenation of the original state and noise

Initialize with:

$$\begin{aligned}\hat{x}_0 &= E\{x_0\} \\ P_0 &= E\{(x_0 - \hat{x}_0)(x_0 - \hat{x}_0)^T\} \\ \hat{x}_0^a = E\{x_0^a\} &= [\hat{x}_0^T \; 0 \; 0]^T\end{aligned}$$

$$P_0^a = E\{(x_0^a - \hat{x}_0^a)(x_0^a - \hat{x}_0^a)^T\} = \begin{bmatrix} P_0 & 0 & 0 \\ 0 & P_v & 0 \\ 0 & 0 & P_n \end{bmatrix}$$

For $k \in \{1, ..., \infty\}$,
Calculate sigma points:

$$X_{k-1}^a = [\hat{x}_{k-1}^a \quad \hat{x}_{k-1}^a \pm \sqrt{(L+\lambda)P_{k-1}^a}]$$

Time update:

$$\begin{aligned}X_{k|k-1}^x &= F(X_{k-1}^x, X_{k-1}^v) \\ \hat{x}_k^- &= \sum_{i=0}^{2L} W_i^{(m)} X_{i,k|k-1}^x \\ P_k^- &= \sum_{i=0}^{2L} W_i^{(c)} [X_{i,k|k-1}^x - \hat{x}_k^-][X_{i,k|k-1}^x - \hat{x}_k^-]^T \\ Y_{k|k-1} &= H(X_{k|k-1}^x, X_{k-1}^n) \\ \hat{y}_k^- &= \sum_{i=0}^{2L} W_i^{(m)} Y_{i,k|k-1}\end{aligned}$$

Measurement update equations:

$$\begin{aligned}P_{\tilde{y}_k \tilde{y}_k} &= \sum_{i=0}^{2L} W_i^{(c)} [Y_{i,k|k-1} - \hat{y}_k^-][Y_{i,k|k-1} - \hat{y}_k^-]^T \\ P_{x_k y_k} &= \sum_{i=0}^{2L} W_i^{(c)} [X_{i,k|k-1} - \hat{x}_k^-][Y_{i,k|k-1} - \hat{y}_k^-]^T \\ K_k &= P_{x_k y_k} P_{\tilde{y}_k \tilde{y}_k}^{-1} \\ \hat{x}_k &= \hat{x}_k^- + K(y_k - \hat{y}_k^-) \\ P_k &= P_k^- - K P_{\tilde{y}_k \tilde{y}_k} K^T\end{aligned}$$

where, $x^a = [x^T \; v^T \; n^T]^T$, $X^a = [(X^x)^T \; (X^v)^T \; (X^n)^T]^T$, λ = composite scaling parameter, L = dimesion of augmented state, P_v = process noise cov., P_v = measurement noise cov., W_i = weights as calculated in equation 3.20.

Figure 3.2: Unscented Kalman Filter Equations and Algorithm, copied from [14]

variables: $x_k^a = [x_k^T v_k^T n_k^T]^T$. The Unscented Transformation sigma point selection scheme (Equation 3.20) is applied to this new augmented state RV to calculate the corresponding sigma matrix, X_k^a. The UKF equations, directly taken from [14], are given in the algorithm of figure 3.2. Note that no explicit calculation of Jacobians or Hessians are necessary to implement this algorithm. Furthermore, the overall number of computations are the same order as the Extended Kalman Filter.

3.4 The ReBEL library

Even if the implementation of a Kalman Filter is quite straightforward, it has been judged useful to use a library to implement the filters.

The library used is *ReBEL : Recursive Bayesian Estimation Library* [1]

ReBEL is a Matlab toolkit of functions and scripts, designed to facilitate sequential Bayesian inference (estimation) in general state space models. That software consolidates research on new methods for recursive Bayesian estimation and Kalman filtering by Rudolph van der Merwe and Eric A. Wan. The code is developed and maintained by Rudolph van der Merwe at the OGI School of Science & Engineering at OHSU (Oregon Health & Science University). That library is free for academic use.

In order to allow the understanding of how the filters have been implemented a rapid overview of how the library works will be presented, with focus on the parts to be defined by the user.

The corner stone on which the library is build is a model structure (called GSSM for General State Space Model) containing a complete description of the system through parameters and functions. The first step to use the library is to define such a model. A small initialisation is required before the filter call. The last step consists of plotting the results.

3.4.1 The General State Space Model

The model contains a lot of parameters but in our specific case only the most important are used. For example, since no linearization of the model is needed in the algorithm, no information about that has to be included in the model. Complete details about the model can be found in the library documentation or by looking at some proposed examples. The 3 parts where the user has to pay the most attention are :

- **Size and noise parameters.** The size information is necessary just to let other functions know how many states, inputs and measurements the system has. The noise definition is a very important part of the model.

[1] http://choosh.ece.ogi.edu/rebel/

Both process and measurement noise are defined here. Each time zero mean Gaussian noise is used and the covariance matrix has to be provided.

- **Next state function.** The function *ffun* takes the previous state as well as the input and the parameters and outputs the predicted state one time step ahead. This function can be nonlinear. In the case when many states (sigma points) have to pass through that function, like in the Unscented Kalman Filter, a loop is created inside and the equations are computed for each point individually. To make the function more readable, the first step always consists in extracting the components of the state, input and parameter into variables with understandable names. The last step is then obviously the concatenation of the modified variables into the new state vector. Those 2 steps are skipped in the description of the function in later chapters. The header of the function looks like :

```
function new_state = ffun(model, state, V, U1)

% FFUN  State transition function (system dynamics).
%
%   Generates the next state of the system NEW_STATE given
%   the current STATE, exogenous input U1 and process noise term V.
%   MODEL is a GSSM derived data structure describing the system
```

- **Observation function.** The function *hfun* gives the predicted measurement from the state, inputs and parameters. Again, this function can be nonlinear and a loop is defined inside to handle the case when many points should go through. The same considerations about the first and last steps for readability apply here also. The header is :

```
function observ = hfun(model, state, N, U2)

% HFUN  State observation function.
%
%   Generates the current possibly nonlinear observation of the
%   system state, OBSERV, given the current STATE, exogenous input U
%   and observation noise term V.
%   MODEL is a GSSM derived data structure describing the system.
```

3.4.2 Initialization

This part is not difficult and quite close to the examples given with library. However the code in itself is quite long. A pseudo version of the code with the main steps is presented here :

- **Import the data from the Dymola result file.** For example

```
Data = dymload('DoubleLaneChangeAndBraking')
v_x = dymget(Data, 'vehicle.chassis.summary.v_x');
```

- **Create the parameter, input, output, and exact state vectors.** The exact state is only used for the state initialisation in the filter and for comparison with the estimated results.

- **Interpolate the data.** Since the solver used in Dymola works with a time varying time step, an interpolation is necessary. A specific interpolation function is needed because of the instantaneous changes in the hybrid variables.

- **Initialization of the GSSM model.** By calling the *init* part of the model, the full structure will be created and the model will be ready for simulation.

- **Create the noise and integrate it in the model.**

- **Initialize the state and the covariance matrix.** Usually the exact state at time zero is used for state initialization and a simple unitary diagonal matrix defines the covariance matrix.

- **Define some specific filter parameters.** In the case of the UKF, the parameters and values are $\alpha = 1$, $\beta = 2$ and $\kappa = 0$.

Chapter 4

State of the art of tire-road friction estimation

The tire-road friction estimation is a very large research area and many different approaches have already been proposed in the literature. Figure 4.1 tries to give a good overview of the main directions taken by the researchers.

As the top branch of Figure 4.1 shows, tire-road friction estimation research can roughly be divided into "cause-based" approaches and "effect-based" approaches. "Cause-based" strategies try to measure factors that lead to changes in friction and then attempt to predict what μ_{max} will be based on past experience or friction models. "Effect-based" approaches, on the other hand, measure the effects that friction (and especially reduced friction) has on the vehicle or tires during driving; they then attempt to extrapolate what the limit friction will be based on this data.

For example, if a human driver sees ice on the road and uses past experience to conclude that the road will be slippery, he is using a cause-based μ_{max} estimation strategy. If he does not see the ice, spins his tires while accelerating, and then concludes that the road must be slippery, then he is using an effect-based estimation strategy.

4.1 Cause-based friction prediction

Numerous parameters "cause" the maximum available friction μ_{max} to be a certain value. In [18], Bachmann classifies them as *vehicle parameters* like speed, camber angle, and wheel load; *tire parameters* like material, tire type, tread depth, and inflation pressure; *road lubricant parameters* like type (water, snow, ice, oil), depth, and temperature; and *road parameters* like road type, microgeometry, macro-geometry, and drainage capacity. A cause-based μ_{max} predictor must be able to measure the most significant friction parameters and then produce an estimate of μ_{max} from a database with information about the effects of

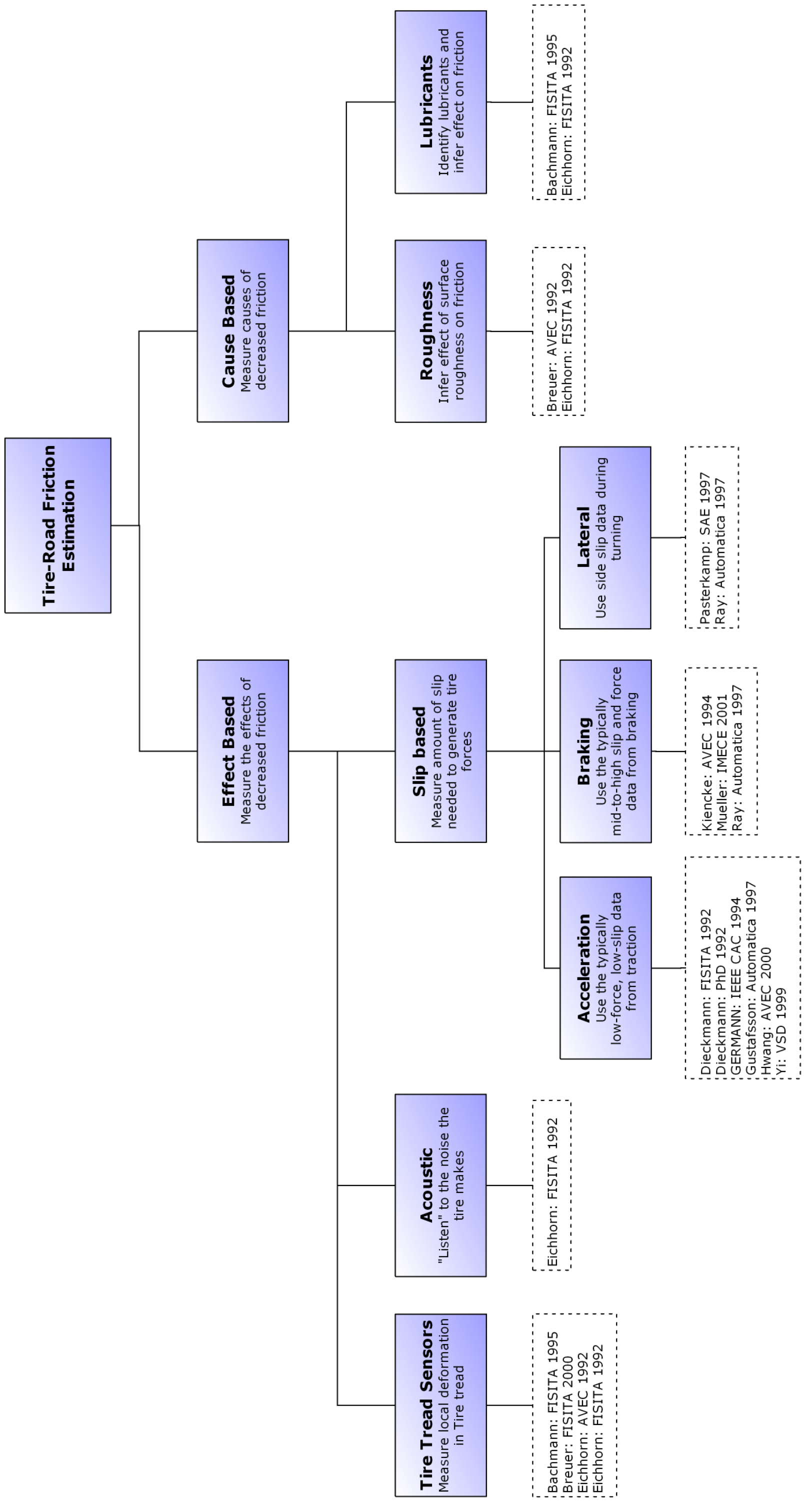

Figure 4.1: A sampling of tire-road friction estimation research. Complete reference information in bibliography or in [7]

these parameters on friction. Many of the parameters affecting μ_{max} are easily determined - for example, speed, tire type, approximate wheel load, and camber. However, measuring two of the parameters that significantly affect friction — lubricant and road type — requires special sensors. This need for extra sensors is one of the main disadvantages of cause-based friction estimation approaches.

As the "Lubricants" branch of Figure 4.1 shows, several researchers have built special lubricant sensors for friction estimation. The optical sensors described in [20] and [19] can detect water films and other lubricants by examining how the road scatters and absorbs light directed at it. Optical sensors have also been constructed to detect the road surface roughness characteristics [19].

Once the parameters affecting friction are known, they must be passed into a friction model of some sort to obtain a μ_{max} prediction. This friction model could be theoretical or physically based, but many researchers have suggested using neural networks and other learning algorithms instead. In [20], for example, the μ_{max} prediction software uses data interpolation, associative storage, and system identification techniques. The disadvantage of this type of nonphysical model is that it loses accuracy when conditions deviate from the conditions under which it was "trained." Nevertheless, experimental results have shown that cause-based μ_{max} estimators can often deliver high accuracy. For example in [20], a cause-based method using data from a wetness sensor and a surface roughness sensor gives a μ_{max} estimate that is within 0.1 of the real value of μ_{max} in 92% of experiments. Since the key sensors were optical, these results were obtained with zero friction demand. That is, the driver did not need to achieve high levels of μ to get a useful estimate of μ_{max}.

As we mentioned above, though, these advantages of good accuracy and zero friction demand come with three main disadvantages: First, cause-based systems often require extra sensors. Second, they may need extensive "training" to work properly. Third, they may have difficulties accurately predicting friction under exceptional conditions for which they have neither sensors nor training.

4.2 Effect-based friction prediction

As Figure 4.1 shows, researchers have pursued at least three types of "effect-based" μ_{max} estimators: acoustic approaches, tire-tread deformation approaches, and slip-based approaches. We briefly review here the acoustic and tire-tread approaches before focussing on the slip-based methods.

In an acoustic approach, a microphone is mounted to "listen" to the tire, and the sound that the tire makes is used to infer something about μ_{max}. According to [20] and [19], the tire noise correlates with the friction demand and deformation of the tire tread, so it is an effect of tire-road friction. At the same time, though, these authors show that the noise is also correlated with parameters that affect friction such as road type, presence of water, and speed. Thus, tire noise indicates something about both the causes and the effects of tire-road friction, so it could have just as easily been classified as a cause-based approach. Regardless of how one classifies this approach, the complex nature of tire noise makes it difficult to use for predicting μ_{max} [20].

The tire-tread deformation approach uses sensors embedded into the tire tread to measure the x, y, and z deformations of the tread as a function of its position in the road-tire contact patch. These deformations are the direct result of x, y, and z force transmission in the contact patch and therefore contain information about the total longitudinal, lateral, and normal forces as well as their geometric distributions in the contact patch. This is useful for estimating μ_{max} because individual tire tread elements often exceed the holding power of the road long before the tire as a whole exceeds μ_{max} and starts sliding. Thus, we see the effects of the μ_{max} limit on the tire before we see its effect on vehicle performance. For example, even in a free-rolling tire, the tread deforms in the longitudinal direction as it flattens to enter the contact patch and then re-takes its natural shape on exiting. The shear stresses associated with this free-rolling deformation can be quite large — as much as 100 kPa, compared to normal pressures on the order of 200 kPa. If the road-tire interface is unable to provide enough adhesive force because μ_{max} is small, certain parts of the contact patch may slide slightly, leading to changes in the tread deformation geometry that are correlated with μ_{max}. When friction demand is non-zero, one might expect even more local sliding in the contact patch, potentially providing more information about μ_{max}.

References [20] and [19] describe a tire-tread deformation sensor and give experimental results for a μ_{max} estimator that uses tread deformation. The sensor consists of a magnet vulcanized into the tread of a kevlar-belted tire (to avoid signal distortion from a steel belt) and a detector fixed to the inner surface of the tire. Experiments using this apparatus show that even with zero friction demand it is possible to detect very low μ_{max} surfaces from tire-tread deformation data. Furthermore, the system does not need to know why the road is slippery to work since it only measures the effects of low μ_{max}. Thus, it is immune to many of the problems of cause-based μ_{max} identifiers. While very promising, this approach has the disadvantage that it requires a sophisticated instrumented tire with a self-powered, wireless data link to the vehicle. Although such links have been successfully tested, they still appear to be several years in the future on production vehicles.

It is primarily the desire to avoid this type of new instrumentation that makes the third effect-based approach — the slip-based approach — so attractive. Taken together, results from the fairly small number of efforts to use slip to classify roads indicate that it may be possible to use tire slip to classify roads into at least two or three friction levels without having to use dedicated sensors. Most of the algorithms in the literature make use of little more than standard ABS wheel speed sensors, and possibly some of the sensors found on vehicles equipped with "Vehicle Dynamics Control" systems.

4.2.1 Slip methods

The basic idea of the slip methods is to use logged data to estimate the friction curve or at least interesting portions of it. To get a point on the friction curve, many values are needed :

- the present slip
- the normal force on the road
- the friction force.

Those values are not trivial to get. We will come back on the estimation of the slip and of the vertical force later. However we can already note that in most cases quite good slip estimation can be obtained if a slow varying bias is allowed. This comes from the uncertainty on the tire radius.

Concerning the friction forces, different approaches have been proposed. The most general one is to use an observer to estimate continuously the forces on each wheel. That idea has been proposed by Ray [8] and followed up by Wilkin [9]. A longer description as well as an implementation and comments are proposed in a later section.

Another widely used possibility is to restrict the time while the forces are available to specific manoeuvres like acceleration, braking or cornering. Gustafsson [11] proposed to use an engine map to get a value of the driving torque in case of normal driving. Some other authors have tried the use the brake pressure to estimate the braking torque but it seems that the measurement does not give very accurate results [7].

Clearly it seems that it is easier to estimate the friction forces during normal condition like driving. However the slip during such conditions stays very small and it is therefore quite difficult to get an accurate idea of the shape of the friction curve. On the other hand, braking occurs less often but provide much higher slips which are better for the identification.

Once the friction force is available an algorithm could be defined to shape the friction force. Most of the proposed approaches use a linear regression to estimate the longitudinal stiffness as well as the slip bias mentioned above. Such a method is presented in Gustafsson [11] using a Kalman filter coupled to a change detector. We will come back to such an algorithm. Other authors like in [21] propose a polynomial fit of the curve. Such an approach give more accurate value for μ_{max} provided that large enough slips can be used in the regression, which is not easy to get in normal conditions.

In the following sections of this report, we look in more detail at some ideas proposed in the field of slip-based friction estimation. Then new approaches, still slip-based, are proposed and analysed.

Chapter 5

Friction force observation using a Kalman Filter

The purpose of this section is to analyse an observer for the friction forces as proposed by Ray [8] and followed by Wilkin [9].

In the background section, a vehicle model has been presented and those 3 equations link the total measurable accelerations and yaw rate (consequences) to the friction forces developed at each tire (causes). The idea is to use a Kalman Filter to reconstruct the causes from the consequences, the forces from the movements.

5.1 Model and filter equations

Let's have a look again at the equations :

$$\begin{aligned}
a_x &= \frac{1}{m}[((Fx_{\text{fl}} + Fx_{\text{fr}})\cos(\delta)) - ((Fy_{\text{fl}} + Fy_{\text{fr}})\sin(\delta)) + (Fx_{\text{rl}} + Fx_{\text{rr}})] \\
a_y &= \frac{1}{m}[((Fx_{\text{fl}} + Fx_{\text{fr}})\sin(\delta)) + ((Fy_{\text{fl}} + Fy_{\text{fr}})\cos(\delta)) + (Fy_{\text{rl}} + Fy_{\text{rr}})] \\
\frac{dr}{dt} &= \frac{1}{Izz}[((Fx_{\text{fl}} + Fx_{\text{fr}})a\sin(\delta)) + ((Fy_{\text{fl}} + Fy_{\text{fr}})a\cos(\delta)) - \\
&\quad (Fy_{\text{rl}} + Fy_{\text{rr}})b - ((Fx_{\text{fl}} - Fx_{\text{fr}})\cos(\delta))\frac{tf}{2} - ((Fx_{\text{rl}} - Fx_{\text{rr}}))\frac{tr}{2})
\end{aligned}$$

From this model, a Kalman Filter can be developed using the following form for the state and measurement equations:

$$\dot{\hat{x}} = f(\hat{x}, \hat{F}, u) \tag{5.1}$$

$$\hat{y} = h(\hat{x}, \hat{F}, u) \tag{5.2}$$

$\hat{x}$ is the estimated state vector, $\hat{y}$ is the reconstructed output, u is the input vector and $\hat{F}$ are the eight estimated forces. More precisely:

$$u = [\delta] \tag{5.3}$$

$$x = [v_x, v_y, r]^T \tag{5.4}$$

$$y = [a_x, a_y, r]^T \tag{5.5}$$

Here the forces are considered as parameters that have to be estimated at the same time as the state. They will therefore be included directly in the state vector. As parameters, they have no dynamics and are modelled with a derivative equal to a random noise.

Since the model is nonlinear a traditional Kalman Filter is not suitable. The filter proposed in the paper is the Extended Kalman Filter where the basic idea is to linearize the equations at each step around the present estimated point. In this thesis another method called the Unscented Kalman Filter, described in section 3.3 and which do not require the linearization, is used.

5.2 Details of the implementation and results

In the first paper proposing the observer (Ray [8]), 7 equations constitute the model. The 3 first ones are the basic ones described above and 4 others are added using the applied torque on each wheel. Since the applied torque is very difficult to measure in practice and would at least require expensive extra sensors, Wilkin [9] only uses the 3 general equation. Of course, many other relations can be found in the car linking the forces to some dynamics and some addition of new relations will be investigated later.

5.2.1 Using the applied torque

As said before, Ray [8] uses measures of the applied torques as inputs to the model and that leads to the addition of the following process equation for each wheel i:

$$\dot{W}_i = (Fx_i R - T_i)\frac{1}{I_w} \tag{5.6}$$

Where T_i is the torque applied and I_w is the wheel's inertia.

The model implementation follow the sketch presented in section 3.4. The main part of the functions `ffun` and `hfun` are given below. The dots represent skipped code; in this case the extraction of the variables from the state, input and parameter vector. The first lines present the forming of the data vectors.

```
params = [m a b tf Izz Rw Iw];                  % Parameters
U1 = [steer, T_fl, T_fr, T_rl, T_rr]';          % Input
y = [a_x, a_y, r, w_fl, w_fr, w_rl, w_rr]'; % Output
Xexact = [v_x v_y r fx_fl fx_fr fx_rl fx_rr fy_fl fy_fr fy_rl
          fy_rr w_fl w_fr w_rl w_rr]';          % Exact state


function new_state = ffun(model, state, V, U1)
  for i = 1 : size(state, 2)
    ...
    v_xD = v_y.*r + 1/m*(((fx_fl+fx_fr).*cos(steer)) -
           ((fy_fl+fy_fr).*sin(steer)) + (fx_rl + fx_rr));
    v_yD = -v_x.*r + 1/m*(((fx_fl+fx_fr).*sin(steer)) +
           ((fy_fl+fy_fr).*cos(steer)) + (fy_rl + fy_rr));
    rD = (((fx_fl+fx_fr)*a.*sin(steer))+((fy_fl+fy_fr)*a.*cos(steer))-
         (fy_rl+fy_rr)*b-((fx_fl-fx_fr).*cos(steer))*tf/2-
         ((fx_rl-fx_rr))*tr/2)/Izz;

    w_flD = -(fx_fl*Rw + T_fl)/Iw;
    w_frD = -(fx_fr*Rw + T_fr)/Iw;
    w_rlD = -(fx_rl*Rw + T_rl)/Iw;
    w_rrD = -(fx_rr*Rw + T_rr)/Iw;

    new_state(1:3, i) = state(1:3, i) + h*[v_xD; v_yD; rD];
    new_state(4:11, i) = state(4:11, i);
    new_state(12:15, i) = state(12:15, i) + h*[w_flD; w_frD; w_rlD; w_rrD];
  end
  new_state = new_state + V;    % add process noise


function observ = hfun(model, state, N, U2)
  for i = 1 : size(state, 2)
    ...
    a_x = 1/m*(((fx_fl+fx_fr).*cos(steer)) - ((fy_fl+fy_fr)
          .*sin(steer)) + (fx_rl + fx_rr));
    a_y = 1/m*(((fx_fl+fx_fr).*sin(steer)) + ((fy_fl+fy_fr)
          .*cos(steer)) + (fy_rl + fy_rr));
    observ(:, i) = [a_x; a_y; r; w_fl; w_fr; w_rl; w_rr];
  end
  observ = observ + N;          % add measurement noise
```

By running the filter on a Double Lane Change and Braking manoeuvre, we get the results shown on figure 5.1. The two first pictures show the longitudinal forces on the front left and rear right wheels. The two others wheels present a very similar behaviour and are not of interest. Then the sums of the lateral forces for the front and the back are shown. Since the equations always uses the groups $(Fy_{\text{fl}} + Fy_{\text{fr}})$ and $(Fy_{\text{rl}} + Fy_{\text{rr}})$ there is no way to reconstruct the individual forces using this model.

Here we can see that the estimate is quite close from the exact force computed by the simulation. The small negative bias present in the longitudinal forces is caused by the other forces not taken into account in this work : the drag force, the rolling resistance, etc.

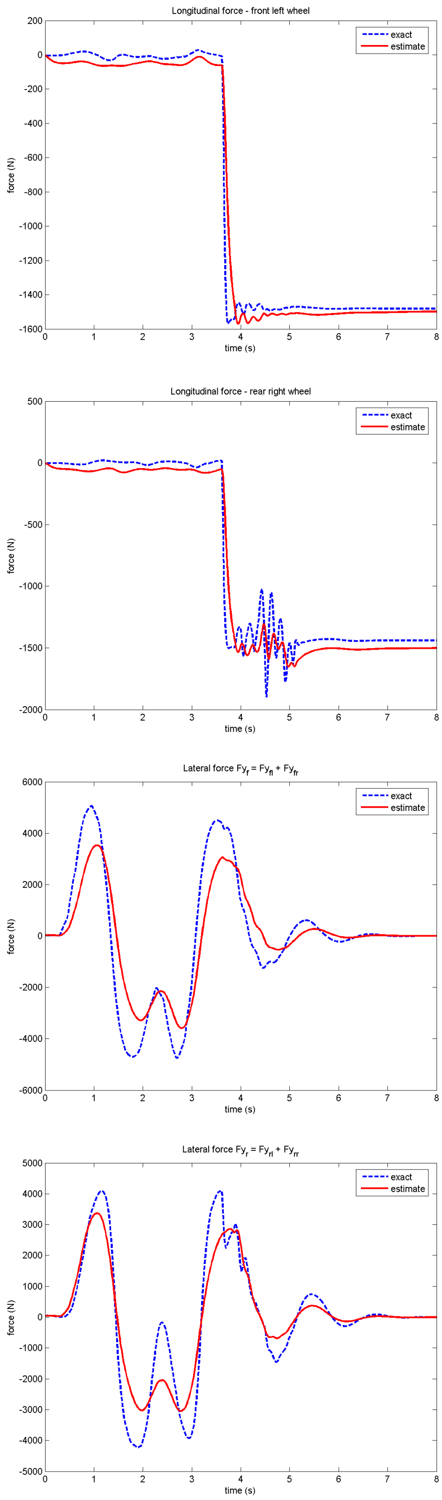

Figure 5.1: Estimated forces for a Double Lane Change and Braking manoeuvre using the applied torque. The results are accurate but require the measurement of the applyed torque, which is not cheap to get in practice.

Analysing closer the equations we notice that the longitudinal friction forces are computed individually using the torque equations. Thus obviously the accuracy of the estimation results from the accuracy of the torque measurement. Since our simulation is noise-free, the estimation is optimal. Then the general equations are used to estimate the two lateral groups. The speeds, not displayed here due to the relatively marginal character, basically come from an integration of the acceleration signal, here again noise-free.

5.2.2 Without the applied torque

Since the torque is difficult to get in practice, we can look at what happen if we only keep the 3 basic equations for which we have all the needed measurements as proposed by Wilkin [9].

The implementation is very similar to the one presented in the previous part.

Running the filter on the same Double Lane Change and Braking manoeuvre, we get the less encouraging results presented on figure 5.2. Again the longitudinal forces for the front left and rear right wheels as well as the groups of lateral forces are displayed.

At the level of the lateral forces, the results from both methods are quite similar since the available equations to observe those forces are identical. However, concerning the longitudinal forces, it really seems that the filter has no way to estimate them properly. Of course the relations used before have been removed at the same time as the torque measurement.

From the beginning, we can question whether the number of equations is enough to estimate so many variables. And unfortunately the answer is close to *no*. In the worse case, we can imagine what would happen for a manoeuvre in straight line. Since the steering angle, the lateral acceleration and the yaw rate are reduced to zero, only one equation is left to estimate the distribution of the total force on the 4 wheels. Even for Tom Cruise this is an Impossible Mission.

A confirmation of our intuition comes from the simulation of the Straight Line Acceleration and Braking manoeuvre as shown on figure 5.3. The observer has no other possibility than divide equally the total force between the 4 wheels even if we know that the distribution is completely asymmetric. So for the braking part where the brake pressure is equally distributed the results looks acceptable; but for the acceleration part this is completely wrong.

So it seems that this approach is clearly too simple and can not give accurate results with a low excitation of the lateral motion. In the paper published on this method, all the tests presented are made using quite extreme manoeuvres on a F1 car. Probably in those cases, do they manage to get enough excitation to improve the estimation? However I have to voice some reservations about the possibility to apply it for everyday driving.

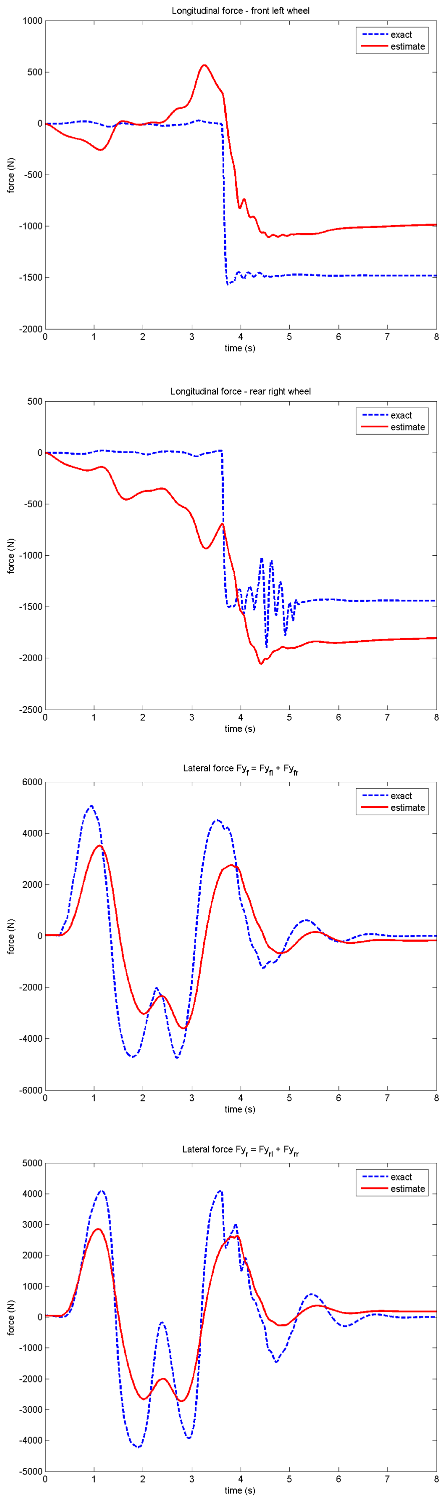

Figure 5.2: Estimated forces for a Double Lane Change and Braking manoeuvre without using the applied torque. Because of the lack of equations, the filter has no way to give an accurate estimate of the longitudinal forces and the chaotic behaviour has no easy explanation.

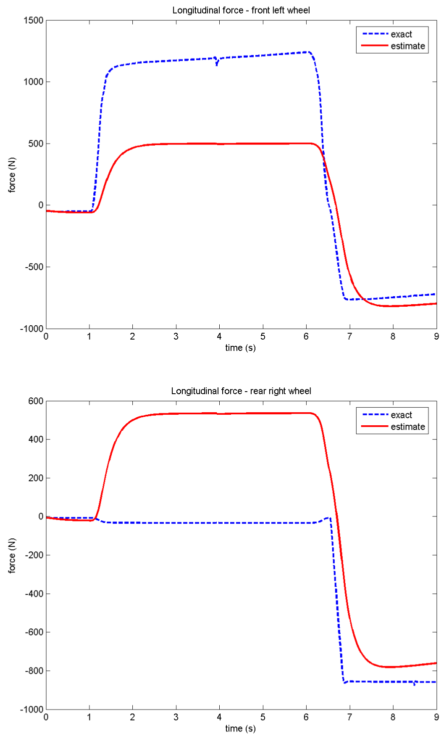

Figure 5.3: Estimated forces for a Straight Line Acceleration and Braking manoeuvre without using the applied torque. Because of the lack of equations, the estimated force on each wheel is simply one quarter of the total force.

5.2.3 Covariance of the noises

The computation of the Kalman gain is a subtle mix between process and observation noise. The less noise in the operation compared to the uncertainty in the model, the more the variables will be adapted to follow the measurements.

Since the forces are not modelled at all, the uncertainty is very high and is represented by a high noise level. On the other hand, since the simulation is noise free, the noise on the observations is said to be quite small. Of course, in a real car, those characteristics could change depending on the specifications of the sensors. The other states modelled using the car's equations or using an integration of the measurements are said to have an average noise.

Chapter 6

Friction estimation for low slip manoeuvre

From the friction forces, assuming we have them, it becomes necessary to develop an algorithm that can give an estimation of the maximum available friction μ_{max}. The method most used in the literature consists of estimation of the slope of the friction curve for low slip.

A lot of articles assure that the slope allows a good classification of the type of road. However, we can note that for the tyre model used in the Vehicle Dynamic Library, this is far from being obvious. The slope of the friction curves at low slip are so close, even for values of the road friction coefficient from 1 down to 0.2, that it is extremely difficult, if not impossible, to determine on what friction we drive. A plot of the friction curves directly extracted from the Bakker Tire Model of the Vehicle Dynamics Library is proposed on figure 6.1. The curves for road friction coefficients of 1, 0.7, 0.5 and 0.2 are displayed.

Without raising doubts about the accuracy of the proposed model, it seems that it is not very suitable for slope change detection. The best way to solve this problem would be to have access to a test vehicle which is absolutely not conceivable in the scope of this work.

Nearly ten years ago, Gustafsson [11] proposed a way to estimate the friction from low slip manoeuvres. This idea has been developed, confirmed by practical test and is now proposed as a functional product sold by the company NIRA Dynamics AB [1].

[1] http://www.niradynamics.se

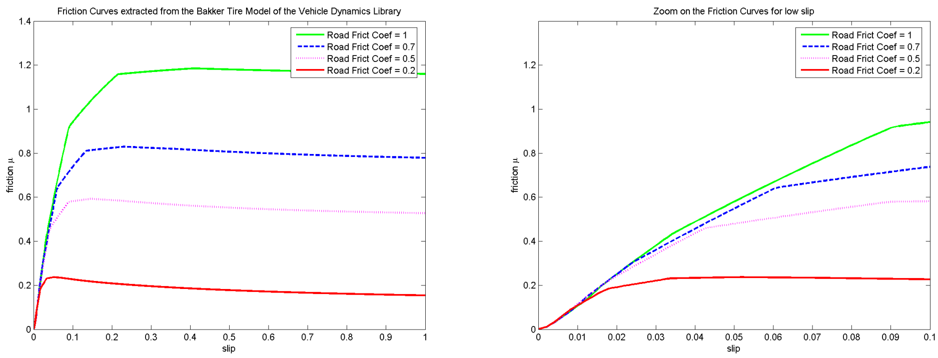

Figure 6.1: Slip Curves extracted from the Bakker Model in the Vehicle Dynamics Library. For various roads, presenting large differences in maximum friction, the longitudinal stiffness (initial slope) are very similar.

6.1 Principle

6.1.1 Friction Forces acquisition

The main idea of this method is to run the algorithm only when it is easy to get the needed information. If we restrict the working time to moments when we are only driving straight (no braking, no too large steering), the longitudinal friction forces on the driving wheels can be estimated using the half of the engine torque, while the forces on the non-driving wheels can be assumed to be negligible. I normal condition, when the engine is not in a transient, the engine torque can be estimated using an engine map stored in the system.

So with such restrictions, friction forces can be acquired quite easily and accurately. Quiet conditions also have the advantage that vertical forces do not vary too much and are therefore easier to model; as well the low lateral forces do not disturb too much the longitudinal friction model.

6.1.2 Linear regression

Using the following relation for low slip

$$\lambda = \mu \frac{1}{C_x} + \Delta \tag{6.1}$$

a Kalman filter can be developed to estimate both $\frac{1}{C_x}$ and Δ. Here Δ is the offset of the slip curve which appears if the value of the slip is biased, like when the effective radius of the wheel is not perfectly known.

The design goal is to get an accurate values on C_x while keeping the possibility to track slow variations in both C_x and δ as well as detect abrupt changes in C_x rapidly. The Kalman Filter is perfect for the slow tracking. However, to overcome the drawback of slow convergence after abrupt changes, a specific CUSUM change detector has been added.

6.2 Limitations and Appreciation

This system really has advantages and drawbacks.

By restricting the sphere of operation of the observer, the estimator is made much easier. This is of course an advantage. As well only a few sensors already available in normal cars are needed. The friction forces obtained are most probably accurate and the points on the slip curves also. This should allow quite good estimation of the low slip behaviour.

Unfortunately, we have seen that low slip behaviour does not always give accurate information about higher slip behaviour; especially since the estimated longitudinal stiffness, used classification, vary a lot because of other parameters not linked to the road. By being unable to use information coming from more exciting manoeuvre, the observer reduces the reachable accuracy and makes large mistakes in specific situations.

It is proved that higher slip is reached while braking than while driving since the decelerations are often faster than the accelerations. Using friction information when braking will clearly improve the μ_{max} estimation. Furthermore an emergency braking with the ABS system turned on will provide very high slip information that could be used to refine the position of the maximum.

Moreover, some applications would benefit from having an estimate of the friction forces, especially in the case of extreme manoeuvres.

However this method gives precious information about the beginning of the curve that could be used to adapt more complicated friction models. As well the ability to estimate the slip bias and therefore the effective wheel radius of the driven wheels while driving can clearly be of first importance for other systems.

So this implementation, already giving interesting results and on which many papers have already been published, has room for further improvements and could be completed by other methods.

Chapter 7

Hybrid observer

An original idea I had and implemented is to use the principle of hybrid observers to choose the best friction coefficient out of a discrete number of possibilities. This approache seems to be very interesting and solving a number of limitations never solved before.

7.1 Principle

In the literature it is very common to try to classify the kind of road we are driving on into a few number of categories like "dry asphalt", "wet asphalt" or "ice" [7] [8] [11]. This tendency leads directly to use hybrid observers instead of continuous ones.

A hybrid system is a system where some parameters are discrete, with a limited number of values. Most of the time, the values influence the general continuous dynamics of the all system. As an example we can look at a gear box where the gear is 1, 2, 3, 4 or 5 but not 2.4. Depending on the engaged gear, the ratio will change and the dynamics of the box will change too. An observer for such a system has been developed by Balluci [15]. Another example is an electronic circuit where the state defines the actions and outputs of the circuit as well as the possible transitions through the state machine.

Many new theories appear to observe such systems. From quite simple to very complex, they try to use as much as possible the available information about the system like the possible transitions of the hybrid variables. One interesting method proposed by Balluci [15] and used in this thesis is to run in parallel a continuous observer for each possible value of the hybrid variable and then select the observer that gives the smallest residual, i.e. the one that explain the best the behaviour of the system.

In our case, the hybrid variable is the road and possible values are the usual categories (or friction coefficients) defined in the literature. The main idea is to compute what should be the friction forces for each type of road defined in the observer, compute what should be the behaviour of the car because of those forces and compare it to the measured behaviour to select the most probable road.

From the beginning, some new functionalities and advantages can be expected from such an idea :

- Non-linear models can be used to describe the friction curves that are obviously non-linear. This allows the estimator to be active in all the situations, even for large slip. The use of nonlinear models is not novel but is really not common in the literature.
- Moreover, the ability to use the information provided by large slip manoeuvres improves the knowledge of the friction coefficient and the maximum of the curve.
- Rapid variations in the friction could be easily detected since the hybrid observers are dedicated to abrupt parameter changes.
- Until now, the steering was considered as a complexity to be moved away since it modifies the friction model. With a non-linear model, the steering does not need to be rejected any more and can even become a good source of excitation for the system.

By looking at the implementation, we will be able to notice that a lot of new problems appear in this approach.

7.2 Implementation

The system has been implemented in Modelica. This kind of implementation is perfect to divide the algorithm in small blocs having a particular function. The general diagram from Dymola is shown on figure 7.1.

On the left the sensors get the information from the car and store them in the main variables used by the algorithm. On the next level, interesting quantities are computed from the raw data. Then an estimate of the forces and of the car's behaviour is done for each possible road. In this case, the different roads are tuned with the friction coefficients 1, 0.7, 0.5 and 0.2. At the end a comparison between the residuals allows the selection of the most probable road.

7.2.1 The sensors

The *wheel sensors* provide a measurement of the angular speed of each wheel. This information is already available in every car equipped with an ABS system.

The *speed sensor* provides an estimate of the longitudinal and lateral speed of the vehicle. A complete description of how to get those speeds is out of the

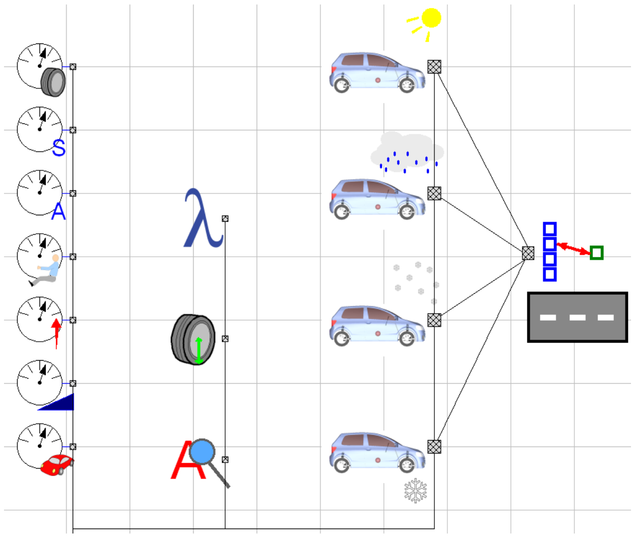

Figure 7.1: Modelica diagram of the Hybrid Observer. The sensors are displayed on the left: wheel speed, car speed, car acceleration, driver instructions, vertical forces, road grade and car parameters. The next level process the data: slip computation, effective tire radius determination and acceleration correction. A car model is simulated for each road condition: sun, rain, snow and ice. Finally, analysis of the residuals allows the selection of the most probable road.

scope of this thesis. However, many works on the subject seems to come close to very nice solutions. One possibility proposed by a team from Stanford [17] is to use the GSP signal received by the car to compute the absolute speed. A measurement of the yaw rate is also included in this bloc. Note that this value is directly available from the ESP system.

The *acceleration sensor* get the values of the longitudinal and lateral accelerations either from an Inertial Measurement Unit (IMU) or from differentiation of the GSP speed signal as proposed by Uchanski [7].

The *driver's instructions sensor* gives a precise measurement of the steering angle as well as qualitative measurements (like on-off) of the clutch, brake and accelerator positions.

The *vertical forces bloc* should provide a good estimate of the load on each wheel. Using information like the accelerations or the pitch and roll movements, a load transfer model can be derived from basic equations of rigid body mechanics. Unfortunately, such a model depends on the mass and the position of the centre of gravity which are quite uncertain. Another source of information that could be investigated is "active suspension" which arrives slowly in the new models and features a deflection measurement of the suspension.

The *road grade sensor* is not directly used in this implementation. However, an empty object appears in the model to keep in mind that such a parameter has to be integrated before implementation in a real car.

Finally, the *vehicle parameters* gives a value to the main parameters describing the behaviour of the vehicle. Some of the parameters like the size of the car are fixed and can therefore be stored forever at the factory. Some others, like the mass, varying along the time, should be estimated. However, a such estimation is out of the scope of this thesis.

7.2.2 Slip computation and wheel radius

A very critical part of the algorithm is the computation of the slip. Assuming the longitudinal and angular speeds are quite well known, the biggest uncertainty lies in the wheel radius.

To be complete it should be noted that the speeds used to compute the slips are those of the contact point and not those of the car body. A correction is necessary as soon as the car is turning. The necessary equations can be found in the Modelica model.

The wheel radius, actually the effective and deformed one, is not known at the beginning and can change depending on the type of tire, the wheel load, the pressure, etc. If an offset is allowed in the slip, like in Gustafsson [11], the radius can be estimated at the same time as the friction curve. Unfortunately the proposed implementation does not really allow such latitude.

The solution proposed to this problem is composed of two parts.

When no torque is applied on the wheel, the slip is very close to zero and therefore the wheel radius can be estimated using

$$R = \frac{V}{\omega}$$

if the speeds are not too small. Such situations happen quite often for the non-driven wheels and happen for the driven wheels while the driver change gears and open the clutch. Those short periods can give a reference for the radius.

Since long periods can occur with always a torque applied, it is necessary to model what should be the variation of the radius around the reference, mainly caused by the change in the load. Using the vertical forces, supposed here to be available (see section 7.2.1), and a standard value for tire vertical stiffness, a good correction can be computed.

In the scope of a project in System Identification [1], dynamic deformations of the radius linked to the internal dynamic of the tire has been investigated. The conclusion is that the best results are obtained if the load and the derivative of the load are taken into consideration for the computation. Higher order models are not better and require much more parameters. However, the introduction of the dynamics does not lead to incredible improvements. Moreover, it has been seen that the dynamics of the tire is non-linear and the coefficients of the dynamics depends on the operating point.

[1] Course taught by Prof Rolf Johansson at the Department of Automatic Control, LTH

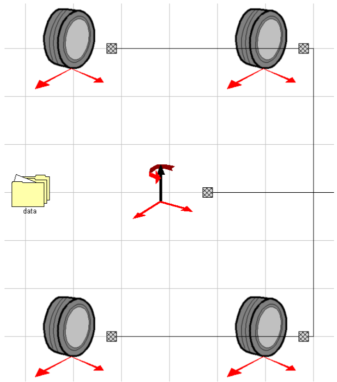

Figure 7.2: Modelica diagram of the Car Model of the Hybrid Observer. The arrows indicate the computed quantities: for each wheel the longitudinal and lateral friction forces, and at the centre the longitudinal, lateral and yaw motion.

Because the stiffness of the tire is very large, a huge load transfer is needed to make a significant change in the radius. Therefore, it has been judged not really worth implementing tire deformations in the details for this first experimentation.

7.2.3 Acceleration Correction

The acceleration of the car body is used to estimate the total force acting on the car. However, this force has other components than only the friction with the road. We can think about the drag force, the gravitation if the grade of the road is not zero, the rolling resistance, etc. Therefore, if possible, a correction of the acceleration to only keep the part due to friction would improve the observer.

To simplify the test in a first time, a perfect correction is applied.

7.2.4 Car model with friction and movements

For each possible road, four in this case, a car model is simulated. The road is set using the road friction parameter. A schematic picture of the model is shown on figure 7.2.

The four wheel models implement a full complex friction model for each wheel based on Pacejka's Magic Formula. Using the slips as input they compute what should be the friction force on the given kind of road. Maybe here the friction model is even too complex and too parameterized. The way the model is implemented will influence a lot the accuracy but also the robustness of the observer. For example the camber property of the tire is present in the model and set to zero since we don't know how to estimate it. The use of a more robust model without camber or the prediction of the camber to be injected in the model would probably improve the observer. Anyway, the idea is more to show that any kind of nonlinear model can be used.

The data element defines all the tire's parameters. Nothing has been investigated in this direction but we could imagine simulating a car with normal tires and another with winter tires since the difference in parameters between the two is quite large. It could be possible to detect both the kind of road and the kind of tire.

The motion model at the centre takes the estimated forces from every wheel and computes the expected accelerations and yaw rate on the given road. By comparing them to the observed values, residuals are generated.

To introduce the Modelica language and give more details about the implementation, the Modelica code of the car model and its components is given below.

```
model CarModel
  parameter Integer j=1 "model's number";
  parameter Real friction = 1 "friction";
  parameter Real a=1 "dist mass center - front axle";
  parameter Real b=1.5 "dist mass center - rear axle";
  parameter Real tf=1.5 "front vehicle track width";
  parameter Real tr=1.5 "rear vehicle track width";
  parameter Real Izz=1300 "Inertial moment around z axis";

  Variables variables;
  FricModel1Wheel fricModel1Wheel1(friction=friction,i=1,j=j,data=data);
  FricModel1Wheel fricModel1Wheel2(friction=friction,i=2,j=j,data=data);
  FricModel1Wheel fricModel1Wheel3(friction=friction,i=3,j=j,data=data);
  FricModel1Wheel fricModel1Wheel4(friction=friction,i=4,j=j,data=data);
  CarsEquations carsEquations(j=j,a=a,b=b,tf=tf,tr=tr,Izz=Izz);
  VehicleDynamics.Vehicles.Chassis.Wheels.ContactForces.MFTyre52.Data.
    Data_205_50_R15 data;

equation
  connect(fricModel1Wheel1.variables, variables);
  connect(fricModel1Wheel2.variables, variables);
  connect(fricModel1Wheel3.variables, variables);
  connect(fricModel1Wheel4.variables, variables);
  connect(carsEquations.variables, variables);
end CarModel;


model FricModel1Wheel
  parameter Real friction=1 "friction";
  parameter Integer i=1 "wheel's number";
  parameter Integer j=1 "model's number";
  parameter VehicleDynamics.Vehicles.Chassis.Wheels.ContactForces.MFTyre52.
    Data.Base data "base for tire data";
  parameter Boolean leftWheel = if (i == 1 or i == 3) then true else false
    "left mounted ?";

  VehicleDynamics.Vehicles.Chassis.Wheels.ContactForces.MFTyre52.Equations
      equationsMFTyre52(data=data) "Magic Formula equations"';
  Variables variables;

protected
  Modelica.Blocks.Math.Gain mirror1(k = if leftWheel then 1 else -1);
  Modelica.Blocks.Math.Gain mirror2(k = if leftWheel then 1 else -1);
```

```
  Modelica.Blocks.Sources.Constant ConstantGamma(k=0);
  Modelica.Blocks.Sources.Constant ConstantFriction(k=friction);

equation
  connect(mirror1.y, equationsMFTyre52.vy);
  connect(ConstantFriction.y, equationsMFTyre52.mue);
  connect(ConstantGamma.y, equationsMFTyre52.gamma);
  connect(variables.V_x[i], equationsMFTyre52.vx);
  connect(variables.V_y[i], mirror1.u);
  connect(variables.w[i], equationsMFTyre52.omega);
  connect(variables.R[i], equationsMFTyre52.Re);
  connect(variables.Fz[i], equationsMFTyre52.fz);
  connect(equationsMFTyre52.fx, variables.Fx[j, i]);
  connect(equationsMFTyre52.fy,mirror2. u);
  connect(mirror2.y, variables.Fy[j, i]);
end FricModel1Wheel;


model CarsEquations
  parameter Integer j=1 "model's number";
  parameter Real a=1 "dist mass center - front axle";
  parameter Real b=1.5 "dist mass center - rear axle";
  parameter Real tf=1.5 "front vehicle track width";
  parameter Real tr=1.5 "rear vehicle track width";
  parameter Real Izz=1300 "Inertial moment around z axis";

  Variables variables;
  SI.Mass m = variables.M "body mass";
  SI.Force fx_fl = variables.Fx[j,1];
  SI.Force fx_fr = variables.Fx[j,2];
  SI.Force fx_rl = variables.Fx[j,3];
  SI.Force fx_rr = variables.Fx[j,4];
  SI.Force fy_fl = variables.Fy[j,1];
  SI.Force fy_fr = variables.Fy[j,2];
  SI.Force fy_rl = variables.Fy[j,3];
  SI.Force fy_rr = variables.Fy[j,4];
  SI.Angle steer = variables.steer;
  SI.Acceleration A_xE "expected longitudinal acceleration for this friction level";
  SI.Acceleration A_yE "expected lateral acceleration"';
  SI.AngularAcceleration DRE "expected yaw rate";

equation
  A_xE = 1/m*(((fx_fl+fx_fr)*cos(steer))-((fy_fl+fy_fr)*sin(steer))+(fx_rl + fx_rr));
  A_yE = 1/m*(((fx_fl+fx_fr)*sin(steer))+((fy_fl+fy_fr)*cos(steer))+(fy_rl + fy_rr));
  DRE = (((fx_fl+fx_fr)*a*sin(steer))+((fy_fl+fy_fr)*a*cos(steer))-(fy_rl+fy_rr)*b-
                  ((fx_fl-fx_fr)*cos(steer))*tf/2-((fx_rl-fx_rr))*tr/2)/Izz;

  variables.resid[j, 1] = A_xE - variables.A_x "longitudinal residual";
  variables.resid[j, 2] = A_yE - variables.A_y "lateral residual";
  variables.resid[j, 3] = DRE - variables.DR "yaw residual";
end CarsEquations;
```

7.3 Results

Placing ourselves in perfect conditions, the system works perfectly fine !

The observer is tested with the Straight Line Acceleration and Braking manoeuvre and the results are plotted on figure 7.3.

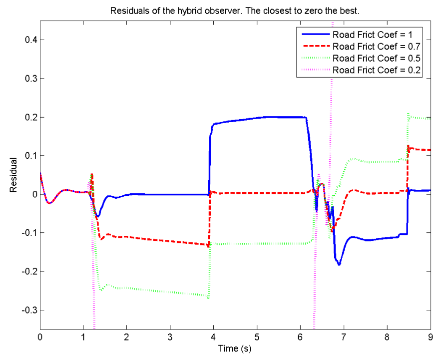

Figure 7.3: Filtering results of the Straight Line Acceleration and Braking manoeuvre using the Hybrid Observer. Between the fourth and eighth second, i.e. during the low friction patch, the residual of the wet road is closer to zero, which indicates a higher probability for that case. The very low excitation, between the sixth and seventh second, explains the chaotic behaviour of the estimator.

It is wonderful to see how, at the change in road friction, the first residual tuned on $\mu_{road} = 1$ will increase and let the second one tuned on $\mu_{road} = 0.7$ come towards zero. This is exactly the expected behaviour of such a system.

Of course, when the excitation is too low, the residuals are superposed and it is not possible to distinguish with one is best. Here also a kind of off function should be applied in such situations.

Unfortunately, the variation of some parameters can make the system completely miss the right answer. Without perfect correction of the acceleration, use of the same tire model, right value for the mass, perfect slip, etc, the observer can gives incorrect estimation.

7.4 Possible improvements

So the system is working but is not robust enough. Unfortunately, in this topic where most of the parameters are really uncertain, this needs to be improved.

First, the variation of the tire parameters, because of the type of tire and the present conditions, has always been a difficult problem to handle in this research area. This is one of the most important sources of wrong estimation. So we can not expect to solve it perfectly. Two ideas in that field could be:

- To take a much simpler tire model with fewer parameters. That way we could expect less sensitivity to uncertainties.
- To adapt the parameters of the model by monitoring some specific values. One possibility would be to look at the maximum and range of longitudinal

stiffness on a long time scale. We could then expect to have some high-grip road during that period.

Furthermore this method is clearly more suitable for high-slip manoeuvres. First because the estimation at low slip is less accurate than some other specific methods; but mainly because this is probably one of the first attempts to use the fully nonlinear friction model. By restricting the estimation to when large enough slip is available, we will certainly reduces the mistakes.

Finally, many researchers are currently working on the estimation of specific quantities intervening in this algorithm. We can expect that with the improvement of those methods, the necessity of robustness will decrease in other applications like this one. This should be the case with values like mass, speed, wheel load, age of the driver, etc.

Chapter 8

Improvement of the Tire Forces Observer

The observer proposed in section 5.2.2 clearly needs the addition of some equations to improve the estimation of the distribution of the friction forces. As well the main topic of this work is the estimation of μ_{max} and therefore the use of a friction model will be somehow needed. In the first section, the introduction of a slip-based friction model directly in the forces observer will be investigated.

As it is always the case in control theory, a feedback loop allows the reduction of the output error while a feedforward speeds up the process. In the second section, an implementation of a feedforward, or a prediction of the dynamics of the variables to be estimated, will be proposed and tested.

8.1 Forces Observer with Linear Friction Model

A general slip-based friction model for the tire can be expressed using the following equation

$$\mu = \frac{Fx}{Fz} = f(\lambda, \theta)$$

Where f is any function, linear or not, of course as close as possible to the exact slip curve and θ is a set of parameters. For example f can have the form of the Magic Formula or more simply be linear with slope C_x.

Using one equation for each wheel and introducing θ in the state to be estimated, we now have enlarged our filter and we can expect improvements.

To be able to use this concept, two assumptions should be made :

All 4 wheels run with the same set of parameters θ. Actually, if this assumption is not made, the number of parameters is so large that an infinite number of possible combinations will satisfy all the equations; the system will be underdetermined. Such assumption is not always valid in everyday driving but moments when it's not satisfied are quite rare.

The slip and the normal forces should be known accurately. In this case, a bias on the wheel's effective radius is not really allowed since the correction would require one parameter for each wheel which is too much as explained in the previous paragraph. More details about this can be found in section 7.2.1.

Looking at Gustafsson's idea presented in previous chapter, I choose to simply implement this idea using a linear friction model described by a single parameter C_x. Practically C_x, or more precisely $\frac{1}{C_x}$, is added in the state vector as a parameter to be estimated. Since the value is quite small and not varying so much — we leave the jump detection to other devices added to the Kalman Filter — the variance of the process noise associated with this parameter is quite low. Four new observation equation are introduced as well — one for each wheel — with the form :

$$\lambda = \frac{1}{C_x}\frac{Fx}{Fz}$$

Since the chosen friction model is linear, it is only valid for low slip and the observer will only be tested on the Straight Line Acceleration and Braking manoeuvre. The results of the test are given on figure 8.1.

Right now the results do not look very impressive. However many nice things can be noticed :

- The estimation of the forces is slightly better now than in the previous case without the friction model.
- More importantly, the estimation of the forces now seems to converge towards the right value which was not the case before. We can expect much better results by speeding up the filter.
- The slope of the friction curve is directly computed. Visibly, the estimation is not perfect. At least it is possible to see a small jump when the road friction change which is encouraging.

A very important remark is that the estimation of C_x becomes completely mad when there is not enough excitation, i.e. when the slips are too low, i.e. when the driver does not request any action. In a practical implementation, the observer should integrate a devise detecting such too low excitation and shutting off the filter.

Since the estimation seems to converge but rather slowly, so, as it is usually done in control theory, a feedforward is integrated.

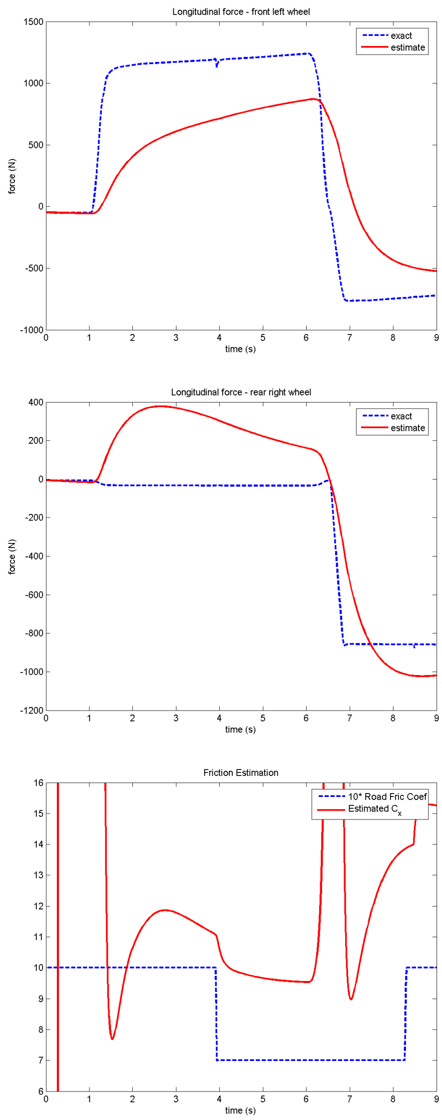

Figure 8.1: Forces and Friction estimation for the Straight Line Acceleration and Braking manoeuvre using a Kalman Filter with linear friction model. The rather slow convergence of the estimated forces can be observed on the first two plots. Between the sixth and seventh second, a very low excitation explains the chaotic behaviour of the estimator. On the last picture, the first curve represents the road friction coefficient and the second curve the estimated longitudinal stiffness. Those two quantities should not be equal but have a similar behaviour.

8.2 Feedforward

Until now no information was directly used to predict the variation of the forces. So they were modelled as static parameters without any specific dynamic. Of course this approach can be improved.

We know that an action on the brakes will induce negative longitudinal forces on each wheel while an acceleration induce positive longitudinal forces on the front wheels only. By looking at some data, it is really easy to identify a simple feedforward.

A good thing about the feedforward is that it is very robust. In other words, since the purpose is only to speed up the convergence at a fast change, it doesn't really matter if the guessed change for one force is really good or not. Of course the better the guess the better the filter will follow the right value. However, a wrong parameter will not destroy the filter. As for every feedforward, a too low guess will require some more time for the filter to adapt while a too high guess will lead to an overshoot.

The results from a test of the improved observer is displayed on figure 8.2.

I really think those results can be said to be really good. The tracking of the forces is very close to the real value for both the acceleration and braking phase. Moreover, the behaviour of the estimated friction slope C_x seems very promising. Jumps occurs exactly when the road friction changes and the slope converge towards similar values on similar roads.

8.3 Appreciation

- Will the slip and the vertical forces really be accurately measurable ?
- Will the cases of too low excitation be possible of handle ?
- Will the jumps in the friction slope be larger in real conditions as suggested by Gustafsson [11] ?
- Is the maximum friction μ_{max} really possible to get from C_x ?

I think that the answers to all those questions are **Yes**. However much more investigations in this direction, coupled with some practical test, are needed to guarantee this positive answer. Unfortunately time and means are always missing.

Clearly, since the friction model used is linear, the filter is restricted to law slip manoeuvres and the same appreciation as for Gustafsson's method applies.

This technique allows the estimation of the friction forces but, on the other hand, less correction parameters can be identified; and it is unlikely that a nonlinear model could be fitted.

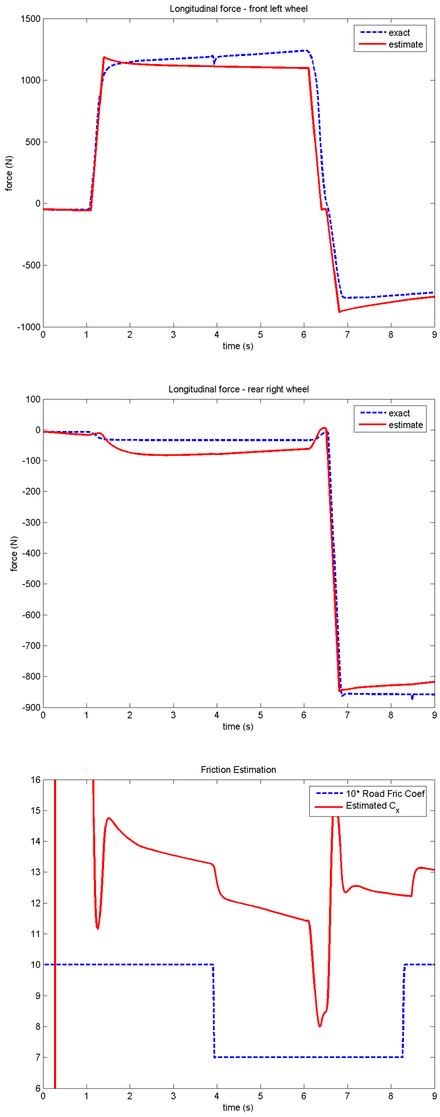

Figure 8.2: Forces and Friction estimation for the Straight Line Acceleration and Braking manoeuvre using a Kalman Filter with linear friction model and feedforward. The convergence towards an accurate value is a lot improved by the feedforward. Between the sixth and seventh second, a very low excitation explains the chaotic behaviour of the estimator. The small difference between the estimated and the exact forces, as well as the slight slope in C_x, is mainly due to the non-modelled drag force.

Chapter 9

Conclusion

Tire-road friction estimation is like a road with icy spots. Many difficulties appear on the way towards the solution and each slippery spot is a challenge to detect and overcome. Unfortunately the problems are not always possible to detect before seeing that the method starts spinning and leading us in a wrong direction. It is therefore necessary to drive carefully which means that the research is not running so fast.

In this thesis, I have focused both on the detection of icy spots on the road and on the detection of slippery points in estimation methods. Published and self-made techniques have been implemented and investigated in the field of slip-based methods.

On the road leading to our final destination, i.e. the estimation of the maximum available friction μ_{max}, three lanes have been traced in this thesis. The first one is simply taken from [11], the second one is an improvement of [9] and the third one is totally home-made.

On the right lane, we find a friction estimator for low-slip manoeuvres. This method works well thanks to its simple principle and can clearly provide extremely useful information. Of course the road classification is already very interesting but the by-products can be as important. By looking at the bias present in the slip calculation, a very good correction can be brought to the tire radius and a rectified value of the slip can be sent to other devices. Unfortunately, obstacles appear on the way as soon as the driver starts braking or steering. Moreover the linearity of the model restricts the use to low-slip manoeuvres. Since the longitudinal stiffness changes because of conditions external to the road, the estimation of the friction peak can easily be wrong.

The centre lane contains a force observer including a linear friction model. Thanks to the ability to estimate directly friction forces, this method has a larger scope than the previous one and can be used, for example, while braking. On the other hand, fewer correction parameters can be estimated at the same time and, among others, an unbiased value of the slip is required. Because of the linearity of the friction model, the same obstacles as in the previous case appear.

The left lane is dedicated to a completely new kind of estimator: a hybrid observer. The main advantage of this method is to feature a nonlinear friction model to classify road in a few categories. This allows a use in any situation, and particularly when high-slip is available. Moreover the peak estimation will be greatly improved since the peak is included in the model. Unfortunately, the weak robustness of such a system to tire characteristics calls for further improvements and probably online adaptation.

When there is an obstacle on the road, you can either stop before it or crash. None of the solutions is really good if someone is waiting for you. Neither an undefined nor a wrong value is good if the driver or another embedded system is waiting for friction estimation. However, when the road is constituted of many lanes, the natural reaction is to overtake. With that analogy I think that a good direction to take in the future would be to combine a linear and a nonlinear observer.

From my position, the combination of a linear observer for low-slip manoeuvres with a hybrid nonlinear observer for high-slip and braking manoeuvres seems very interesting and promising. The nonlinear system could take over when the linear one is out of its depth. As well the low-slip information can provide correction and adaptation to the less robust system. Of course, a switching strategy should be developed and new difficulties could show up.

Clearly a lot of work is still to be done in this research area. Probably new techniques will be created within the next few years. Focussing on the proposed methods, future work should take the following directions. A critical part is to increase the robustness of the tire model and investigate how it could be adapted by monitoring some measurable or estimable quantities. Another interesting topic is the investigation of the precision we can expect on the slip computation.

From a personal point of view, this thesis has been fantastic. I had the opportunity to discover a very interesting and motivating topic in automotive control and active safety. All the time I have been free to find and choose the directions of the project. This does not imply that results come faster but it develops research, organisation, synthesis, anticipation and imagination skills. As well, it has been a perfect occasion to apply theoretical knowledge, to deeper understand control and estimation concepts, to familiarize myself with vehicle dynamics and to learn new advanced techniques; all of it in a renowned department and an international environment. To me this thesis really represents the highlight of five years of technical training and personal development.

Bibliography

[1] Georg Rill. Vehicle Dynamics Lecture Notes, Fachhochschule Regensburg, October 2003.

[2] T.D. Gillespie. Fundamental of Vehicle Dynamics. Society of Automotive Engineers, Warrendale, PA, 1992.

[3] H.B. Pacejka. Tyre and Vehicle Dynamics. Butterworth-Heinemann, 2002.

[4] C.R. Carlson & J.C. Gerdes. Nonlinear Estimation of Longitudinal Tire Slip Under Several Driving Conditions. Proceedings of the 2003 American Control Conference, 2003.

[5] Jacob Svendenius. Tire Models for Use in Braking Applications. Licentiate thesis, department of Automatic Control, LTH, Sweden. Nov 2003.

[6] J. Svendenius & B. Wittenmark. Review of Wheel Modeling and Friction Estimation. Internal report, department of Automatic Control, LTH, Sweden. Aug 2003.

[7] M.R. Uchanski. Road Friction Estimation for Automobiles Using Digital Signal Processing Methods. PhD Thesis, University of California, Berkeley, 2001.

[8] Laura R. Ray. Nonlinear Tire Force Estimation and Road Friction Identification: Simulation and Experiments. Automatica, Vol 33, No 10, pp.1819-1833, 1997.

[9] M.A. Wilkin, M.C. Levesley & W.J. Manning. Design and Verification of an Extended Kalman Filter to Estimate Vehicle Tyre Forces. SAE 2006-01-1285, SAE World Congress Detroit Michigan, 2006.

[10] M.A. Wilkin, D.C. Crolla, M.C. Levesley & W.J. Manning. Estimation of Non-Linear Tyre Forces for a Performance Vehicle using an Extended Kalman Filter. SAE 2004-01-3529, Proceedings of the 2004 SAE Motorsports Engineering Conference and Exhibition, 2004.

[11] F. Gustafsson. Estimation and Change Detection of Tire-Road Friction Using the Wheel Slip. IEEE Control Systems Magazine, 1997.

[12] Rolf Johansson. System Modeling and Identification. Prentice Hall, ISBN 0-13-482308-7, Jan 2004.

[13] S.J. Julier & J.K. Uhlmann. A New Extention of the Kalman Filter to Nonlinear Systems. In Proc of Aeroense: the 11th Int. Symp. On Aerospace/Defence Sensing, simulation and controls., 1997.

[14] E.A. Wan & R. van der Merwe. The Unscented Kalman Filter for Nonlinear Estimation. The IEEE 2000 Adaptive Systems for Signal Processing, Communications, and Control Symposium 2000. AS-SPCC. 2000.

[15] A. Balluchi, L. Benvenuti, M. Di Benedetto & A. Sangiovanni. A hybrid observer for the driveline dynamics. Proc 6th European Control Conference, ECC 2001.

[16] A. Balluchi, L. Benvenuti, M. Di Benedetto & A. Sangiovanni. Design of observers for hybrid systems. In: Hybrid Systems : Computation and Control (Claire J. Tomlin and Mark R. Greenstreet, Eds). Vol 2289 of Lecture Notes in Computer Science. Pp. 76-89. Springer-Verlag. Berlin Heidelberg New York.

[17] H.S. Bae, J.Ryu & C. Gerdes, Road Grade and Vehicle Parameter Estimation for Longitudinal Control Using GPS. IEEE Intelligent Transportation Systems, 2001. Proceedings. 2001.

[18] Th. Bachmann. Wechselwirkungen im prozeßder reibung zwischen reifen und fahrbahn. Reihe 12 360, Fortschritt-Berichte VDI, 1998.

[19] Bert Breuer, Ulrich Eichhorn, & Jürgen Roth. Measurement of tyre/road friction ahead of the car and inside the tyre. Proceedings of AVEC92 (International Symposium on Advanced Vehicle Control), pages 347353, 1992.

[20] U. Eichhorn & J. Roth. Prediction and monitoring of tyre/road friction. XXIV FISITA Congress, London, GB, 2:6774, June 7-11 1992. "Safety, the Vehicle, and the Road".

[21] St. Germann, M. Würtenberger, & A. Daiß. Monitoring of the friction coefficient between tyre and road surface. Proceedings of the third IEEE Conference on Control Applications (August 24-26, 1994), 1:613618, 1994.

[22] N. Petersson & M. Santesson. Experimental Slip-based Road Condition Estimation. Master Thesis, Automatic Control department, Lund Institute of Technology, 2000.